

## **The INFLUENCE of BEARING ASYMMETRY on ROTOR STABILITY**

**Edgar J. Gunter, Ph.D.**

**RODYN *Vibration Analysis, Inc.***

***Professor Emeritus Mechanical and Aerospace Engineering***

***Former Director, Rotor Dynamics Laboratory, Univ. Of Virginia***

***Fellow ASME***

**DrGunter@aol.com**

### **Abstract**

This paper deals with the influence of bearing asymmetry on the stability characteristics of a rotor under the influence of internal friction and aerodynamic cross coupling forces. The Jeffcott rotor is first examined for stability under each of these excitation mechanisms. It is seen that bearing asymmetry plays an important role in improving rotor stability. Of great importance, however is the relationship of the vertical bearing stiffness to the shaft stiffness. When the vertical bearing stiffness exceeds the shaft stiffness, then the influence of asymmetry is diminished. Also of importance is the strength of the instability mechanism. As this value increases, then it becomes increasingly difficult to stabilize the rotor through the effects of bearing asymmetry alone. The inclusion of bearing damping is of major importance in order to achieve significant improvements in stability. There is an optimum amount of bearing damping to be used to apply maximum stability. High bearing damping in combination with high bearing stiffness values, however, causes a degradation in rotor stability. The stability of multistage compressors in five pad bearings is examined because of the apparent benefit of these asymmetrical stiffness bearings in improving stability. It will be demonstrated that many previous five pad bearing designs for multistage compressors had serious stability problems because of the excessive vertical stiffness values generated by these bearings with L/D aspect ratios less than one and preloads exceeding 0.3. It will also be shown that improvement in stability may be achieved by the use of the 5 pad bearing with reduced preloads or by the use of the 4 pad load between pad bearing design with extended bearing aspect ratios. This design approach usually eliminates the need for a squeeze film damper which is required in many of the previous rotor designs using 5 pad bearings.

## **Background and Introduction**

The use of the tilting pad bearing for compressors and industrial turbines has led to significant improvements in turbomachinery performance and operating speeds. As compressor designs have increased to rotors with impeller stages exceeding 8 and speeds in excess of 10,000 RPM, serious stability problems have been encountered in some high pressure compressors because of the generation of internal Alford type aerodynamic cross coupling forces developed in these machines. This condition is not detected under normal factory low pressure performance runs but occurs under full operating conditions in the field.

The increase in number of stages creates a very flexible rotor design with a reduced critical speed. The higher the operating speed is above the critical speed, the more sensitive is the unit to self excited forces. This leads to the occurrence of fractional frequency whirling of the shaft in which the shaft motion has a large subsynchronous component related to the rotor first critical speed. Although the whirl motion may often appear to be constrained at the bearings, the center span motion may exceed the labyrinth seal clearances causing rubs or even shaft failure.

A detailed report by Smith in 1975 on fractional frequency whirling of a high pressure compressor was reported at the Fourth Annual Turbomachinery Symposium sponsored by Texas A&M University. The 9 stage rotor was operating at speeds in excess of 10,000 RPM and was supported by 5 pad bearings. In an attempt to improve the stability, several bearing modifications were attempted in order to increase the bearing asymmetrical stiffness properties to promote higher stability.

This paper was of considerable interest to the author because the motivation for the bearing modifications was based upon my dissertation and ASME paper on the influence of anisotropic supports on rotor stability. The primary consultant on the project was my thesis advisor from the University of Pennsylvania. It should be noted that a detailed analysis of the rotor bearing stability characteristics was not possible at that time. The Lund programs on tilting pad bearings and complex eigenvalue analysis (damped natural frequencies) were not available for use at that time. In the paper presented by Smith are shown a number of bearing modifications attempted in order to increase the bearing anisotropic properties. These bearing modifications proved to be unsuccessful. A final design incorporating a squeeze film damper was also of limited success as it was improperly designed as a long bearing damper which generated excessive stiffness and damping.

The final design, in order to operate at the higher speeds and pressure ratios, involved a new shaft design with a reduced bearing span and increased shaft diameter. Of interest to note that a later consulting group (using the Lund bearing and stability programs) concluded that the zero preload bearing design would be as good as the installed damper. It was reported that the total cost of the retrofit and production loss exceeded 25 million dollars!

This paper presents how this situation may be avoided in the future by the proper selection of the type of tilting pad bearing, choice of preload and bearing aspect ratio. It is estimated today that fractional frequency whirl problems encountered in multistage compressors supported by the 5 pad bearing configuration has caused hundreds of millions of dollars in costs from redesigns and losses in production.

## Jeffcott Rotor on Rigid Supports

It first will be examined the influence of internal friction on the simple Jeffcott rotor as shown in Fig. 1. The Jeffcott rotor has a single disk of approximately 100 lbs and is mounted on a flexible uniform shaft with a length of 40 in and a diameter of 4 in. The rotor is constrained at the ends with simple supports that provide no damping.

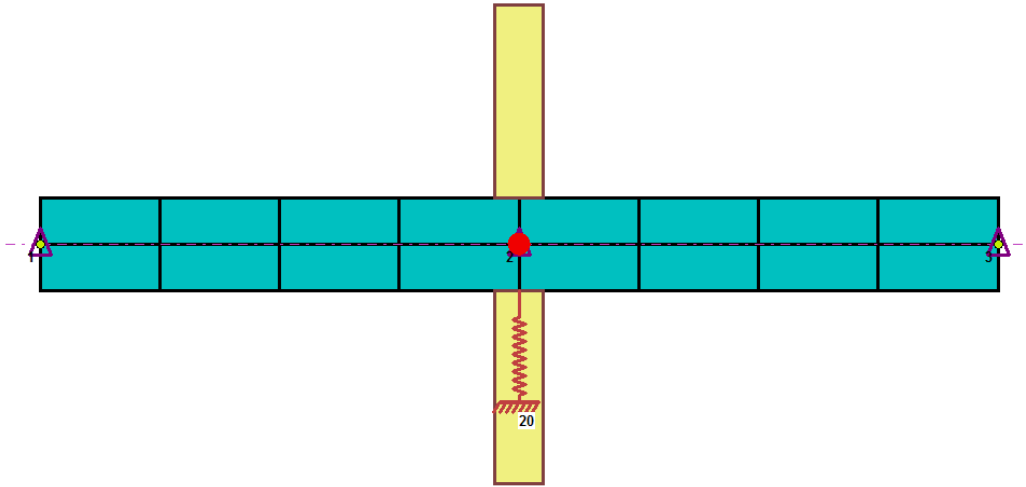


**Fig 1 Jeffcott Rotor on Simple Supports**

The shaft stiffness is given by:

$$K_{shaft} = \frac{48EI}{L^3} \quad (1)$$

The natural frequency of the Jeffcott rotor is given as follows:

$$\omega_{cr} = \sqrt{\frac{K_{shaft}}{M_{modal}}}, \text{ rad / sec} \quad (2)$$

It is of interest to note that a typical 8 stage compressor may be reduced to a Jeffcott model for the purposes of stability analysis by using the modal mass and stiffness generated by a critical speed analysis based on rigid bearing supports. This helps to quickly determine if a particular bearing design may be suitable.

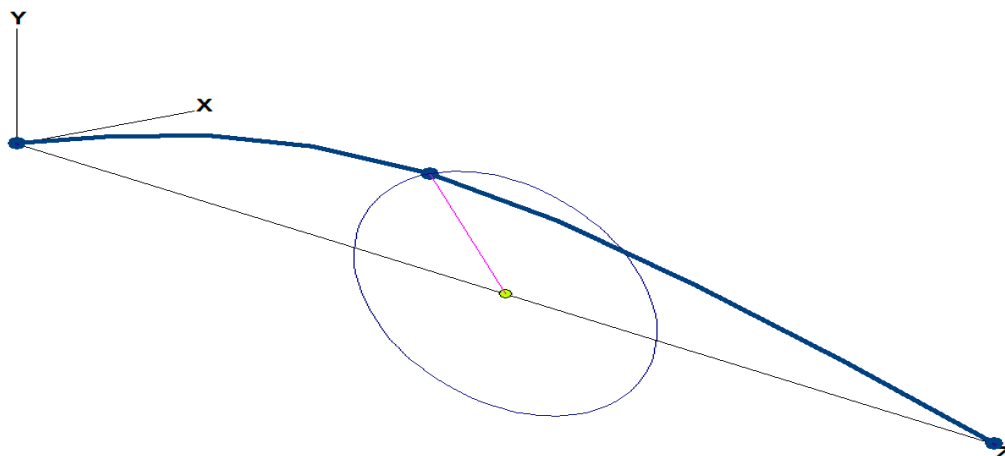


**Fig 2 First Critical Speed Mode Shape of Jeffcott Rotor at 9607 RPM**

Figure 2 represents the first critical speed mode shape of the Jeffcott rotor. Note that the motion is constrained at the bearings. It is interesting to note that most compressor manufacturers place monitoring probes at the bearings to monitor the motion. For the case of very stiff bearings, there will be very little motion observed at the bearing location while the center span is in large amplitude whirling. This can lead to rotor failure without the probes shutting down the system.

### Models of Internal Rotor Friction

There are several models of internal friction that have been used in analysis. The first type of internal friction Model is referred to as hysteretic damping and is give as follows:

$$\vec{F}_{shaft} = -K_{shaft} (1 + i\alpha) \vec{Z} \quad (3)$$

In this model the internal hysteretic damping is independent of frequency. The value of alpha is small in comparison to unity. This effect generates a force perpendicular to the displacement vector.

The model of internal friction that will be employed is the viscous friction model as shown below.

$$\vec{F}_{shaft} = -\left(C_i \vec{V}_{rel} + K_{shaft} \vec{Z}\right) \quad (4)$$

In this model, the internal friction is expressed as a function of the relative velocity in a rotating coordinate system. When expressed in terms of Fx and Fy in a fixed coordinate system, as shown in Eq 5, it is seen that the relative damping term generates cross coupling terms of opposite sign in the x and y directions. In general, it is the presence of cross coupling components of opposite sign that generates instability in rotor bearing systems.

$$\begin{aligned} F_x &= -(KX + \omega c_i Y) \\ F_y &= -(KY - \omega c_i X) \end{aligned} \quad (5)$$

### Planar Motion With Internal Friction

If planar motion is assumed with zero shaft rotation, then the equations of motion appear similar to the single mass system with gravity excitation as shown in Eq 6.

$$M\ddot{Y} + C_i \dot{Y} + K_{shaft} Y = -Mg \quad (6)$$

A value of internal damping of Ci equal to 5 Lb-sec/in was chosen. This value represents an amplification factor of Ac=50. For light damping the amplification factor is related to the log decrement as follows:

$$A_c = \frac{1}{2\xi} \approx \frac{\pi}{\delta}; \delta = \log \text{ decrement} \quad (7)$$

The value of the log decrement in this case is 0.0628. A time transient analysis of the nonrotating system under the influence of gravity is shown in Fig. 3. The log decrement is formally defined as the logarithmic ratio of successive amplitudes of motion. In Fig. 3 the maximum deflection of 0.774 mils is twice the static under gravitational loading. The natural frequency may be estimated from the static deflection by the equation  $N_{cr} = 60/(2\pi) \sqrt{g/\delta} = 9.55 \sqrt{g/\delta} = 9539 \text{ CPM}$ .

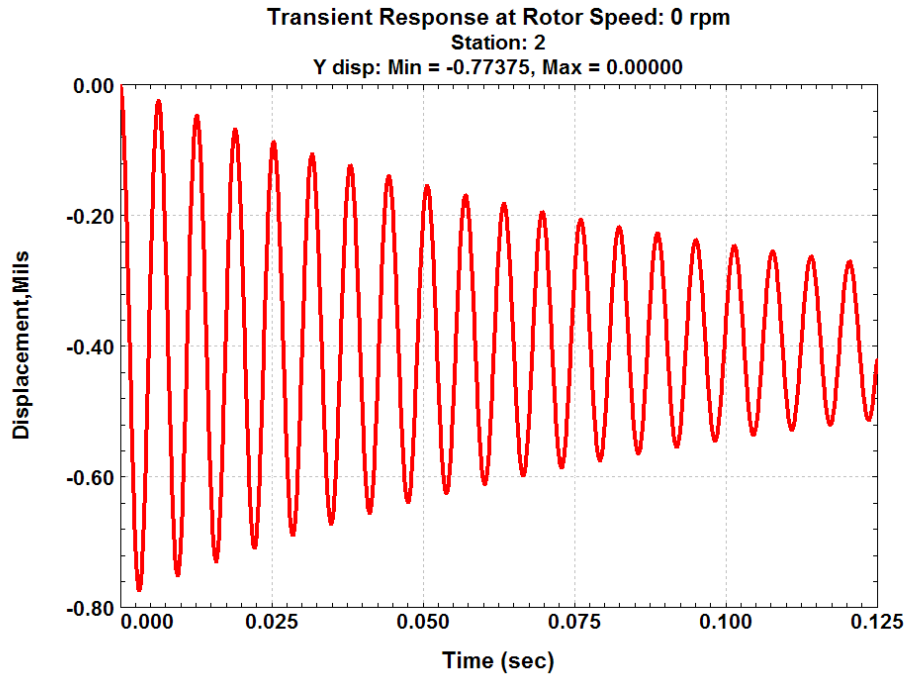


**Fig. 3 Transient Motion of Jeffcott Rotor at Zero Speed With Gravity Excitation**

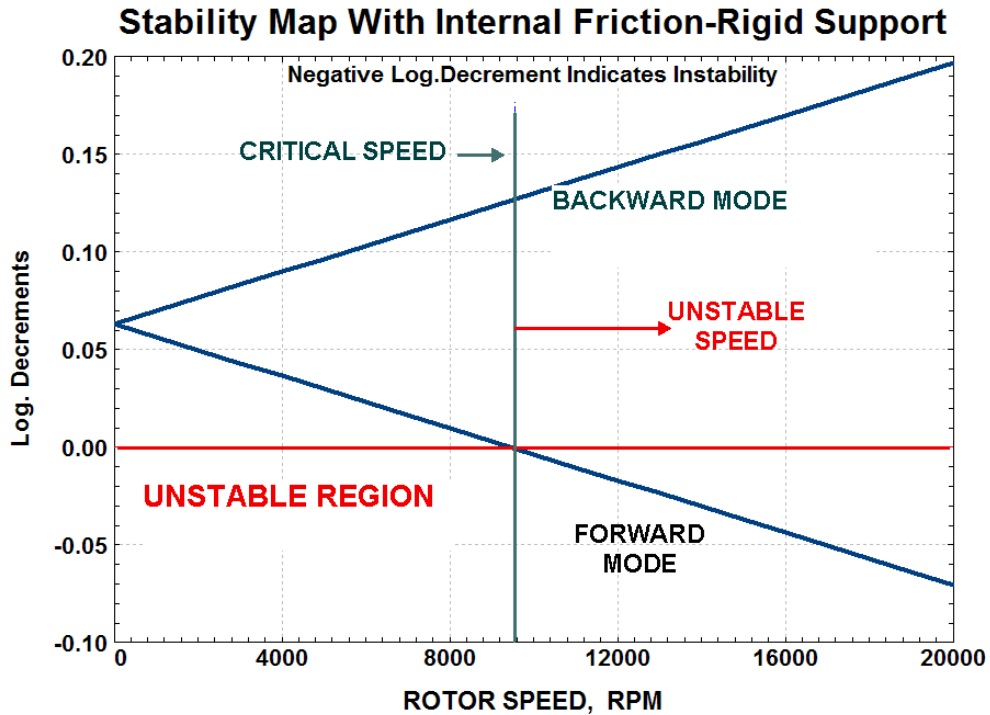
### Stability of Jeffcott Rotor With Internal Friction on Rigid Supports

The stability analysis over a speed range will be computed by the finite element program *DYROBES* which allows for the computation of the system damped eigenvalues and time transient motion. When the earlier studies of this stability mechanism were explored, only the threshold of stability was computed (zero log decrement) using a state of the art UNIVAC digital. The linear and nonlinear time transient motion studies were computed at that time using an analog super computer (which is no longer in existence). Similar and more advanced models may now be computed with finite element techniques and PC computers which have replaced the “super computers” of yesteryear.

Rotor Bearing System Data																	
Axial Forces		Static Loads		Constraints		Misalignments		Shaft Bow		Time Forcing		Harmonic Excitation		Torsional/Axial			
Units/Description		Material		Shaft Elements		Disks		Unbalance		Bearings		Supports		Foundation		User's Elements	
Bearing: 1 of 3		<input type="checkbox"/> Foundation		Add Brg		Del Brg		Previous		Next		Import *.xls		Export *.xls			
Station I: 2		J: 1		Angle: 0													
Type: 1-Speed Dependent Bearing																	
Comment: Internal Shaft Friction																	
	rpm	K <sub>xx</sub>	K <sub>xy</sub>	K <sub>yx</sub>	K <sub>yy</sub>	C <sub>xx</sub>	C <sub>xy</sub>	C <sub>yx</sub>	C <sub>yy</sub>	M <sub>xx</sub>	M <sub>xy</sub>						
1	1000	0	0	0	0	5	0	0	5	0	0						
2	6000	0	3141	-3141	0	5	0	0	5	0	0						
3	8000	0	4678	-4678	0	5	0	0	5	0	0						
4	9000	0	4712	-4712	0	5	0	0	5	0	0						
5	10000	0	5235	-5235	0	5	0	0	5	0	0						
6	12000	0	6283	-6283	0	5	0	0	5	0	0						
7	14000	0	7330	-7330	0	5	0	0	5	0	0						
8	16000	0	8377	-8377	0	5	0	0	5	0	0						
9	20000	0	10471	-10471	0	5	0	0	5	0	0						

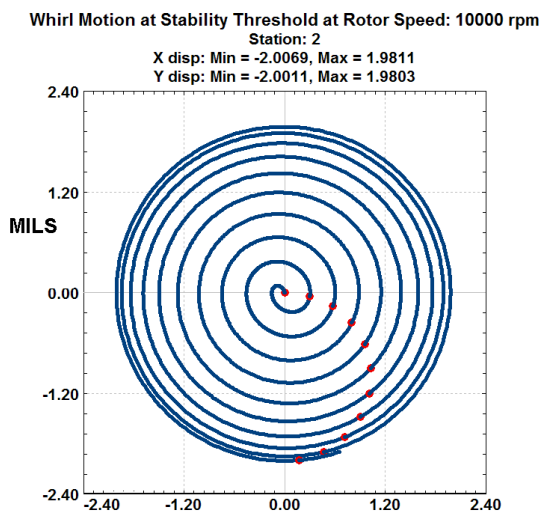
**Table 1 Internal Friction Cross Coupling Stiffness and Damping Coefficients Acting At Rotor Center Over a Speed Range**

Table 1 represents the stiffness and damping coefficients for internal friction acting at the rotor center. Over a speed range from 0 to 20,000 rpm. Note that as speed increases, the cross coupling coefficients increase as give by Eq. 5.



**Fig. 4 Log Decrement of Jeffcott Rotor With Internal Friction With Speed Range Of 0 To 20,000 RPM**

Figure 4 represents. the log decrement vs speed for the Jeffcott rotor. There are two modes shown in the figure. The upper mode is the backward mode. As speed increases, the backward mode log dec increases. Thus internal friction can not cause the system to whirl backwards. The log dec for the forward mode continues to reduce with speed until the critical speed of 9550 RPM is reached. At this point the log dec is zero.. This speed is referred to as the threshold of stability speed. Thus we see that for the classical Jeffcott rotor on fixed supports, the system becomes unstable at speeds above the critical speed.



**Fig. 5 Whirl Motion At 10,000 RPM**

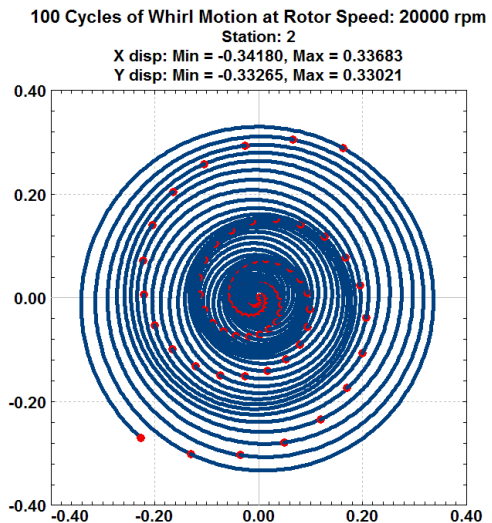


**Fig. 6 Whirl Motion At 20,000 RPM**

## Stability of Jeffcott Rotor With Internal Friction on Undamped Symmetric Supports

Flexible supports will now be added to the Jeffcott rotor as shown below in Fig. 7.. A bearing stiffness of  $K_{xx}=K_{yy} = 125,000$  RPM will now be added to the model.

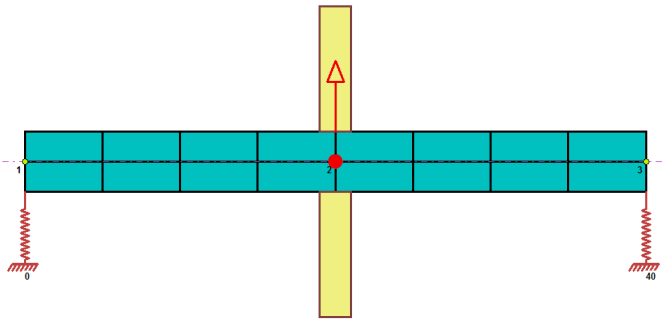


Fig. 7 Jeffcott Rotor With Flexible Supports

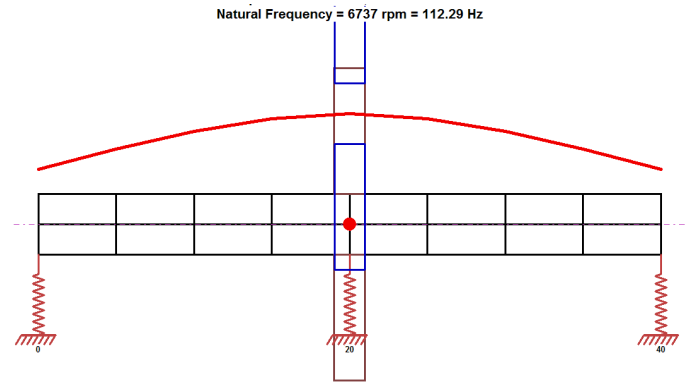


Fig. 8 Critical Speed With  $K_b=125,000$  Lb/in  
 $N_c = 6,737$  RPM

The incorporation of finite bearing support stiffness of 125,000 Lb/In causes a reduction in the critical to  $N_c = 6,737$  RPM. The introduction of a symmetrical support flexibility will not only lower the critical speed, but also cause a reduction in the onset of stability speed. This is the general characteristic of self excited whirling whether caused by fluid film bearings or aerodynamic cross coupling and internal friction. The incorporation of undamped symmetric supports causes a reduction in the critical speeds and lowers the stability threshold. However, when damping is also included, such as a squeeze film damper, the stability may be greatly improved.

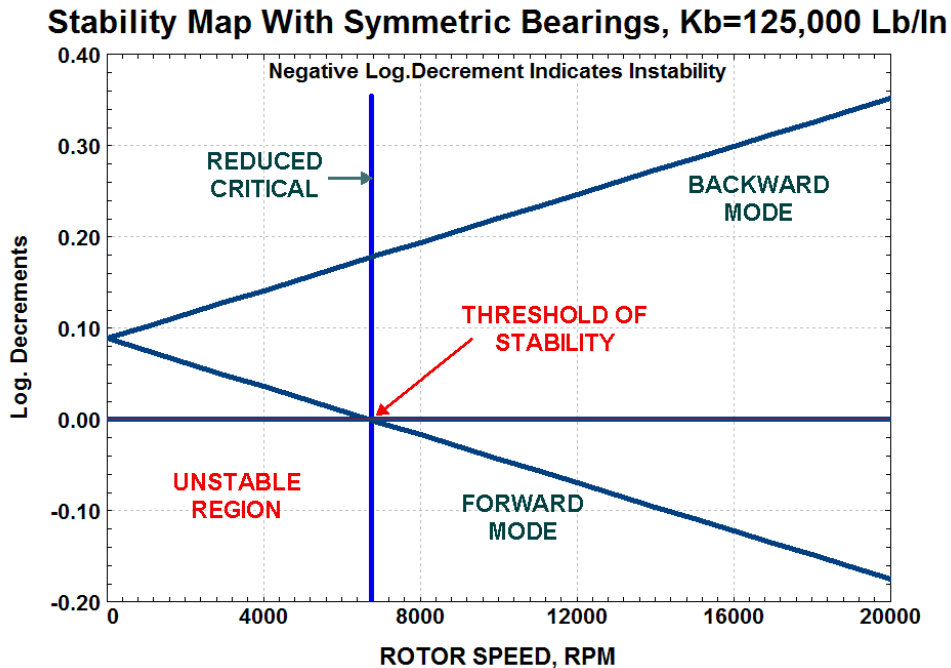
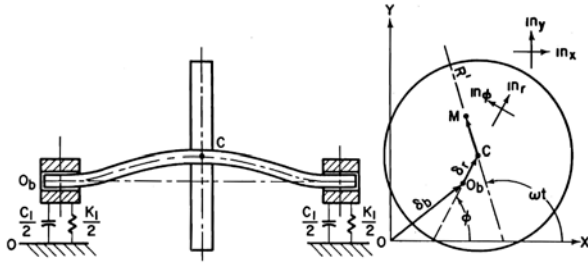


Fig. 9 Log Decrement of Jeffcott Rotor With Internal Friction  
With  $K_b=125,000$  Lb/In For Speed Range of 0 To 20,000 RPM

Figure 9 represents the forward and backward log decrements of the Jeffcott rotor with internal friction with the addition of the flexible bearing supports. In the absence of bearing damping, the forward mode becomes unstable at a lower speed due to the reduction of the critical speed.

## Stability of Jeffcott Rotor With Internal Friction on Damped Symmetric Supports

Figure 10 represents the Jeffcott model with damped symmetric supports. Figure 11 represents the stability map generated for various values of bearing damping. Of interest is the base curve that shows that if we simply incorporate simple flexible supports without damping, the critical speed is reduced and also the threshold of stability. The analysis shows that once the rotor speed exceeds the undamped critical speed, the system becomes unstable under the influence of internal friction.



**Fig. 10 Model of Jeffcott Rotor With Symmetric Damped Supports (Gunter)**

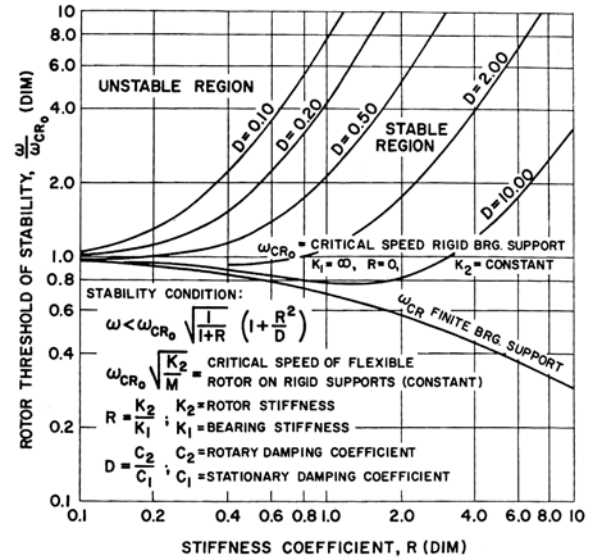


**Fig. 11 Stability Map With Symmetric Damped Support (Gunter)**

In Fig. 11 is shown the influence of support damping  $D$  ratio and the bearing stiffness ratio  $R$  in changing the stability threshold. The simplified stability criterion as shown in Fig. 11 may be expressed as:

$$N_{stability} = N_{cr} \sqrt{\frac{1}{1+R} \left[ 1 + 2R^2 \left( \frac{2C_{brg}}{C_i} \right) \right]} \quad (8)$$

where:  $N_{cr}$  = Critical Speed Rigid Supports

$$R = \frac{K_{sheft}}{2K_{brg}}$$

Figure 11 shows that as the support ratio  $R$  becomes larger than unity (softer support conditions), the stability increases with an increase of bearing or support damping. It should be noted that Eq. 8 is an approximate equation based on small damping values. It will be shown that there is a limit to the amount of effective damping that can be incorporated into the flexible supports to improve stability. As the damping becomes excessive, a point is approached which is referred to as bearing or damper lockup. This occurs with squeeze film dampers with tight clearances and high loading conditions. With excessive support damping, the log decrement no longer continues to increase, but then begins to decrease. When this begins to occur we have passed the point of optimum damping.

Figure 12 shows the mode shape and log decrement with zero support damping at a speed of 20,000 RPM. The system is unstable with a log decrement of -0.1523. The whirl frequency corresponds to the undamped natural frequency of 6,743 CPM. The motion at the bearings is in phase to the motion of the center disk.

Figure 13 represents the system first mode when the bearing or support damping is increased to  $C_b = C_{xx} = C_{yy} = 200$  Lb-Sec/in. The system is now stable with a log decrement of 1.1868. The support damping

has also increased the damped natural frequency from the undamped value of 6,743 CPM to 7,681 CPM. Note that the mode shape is no longer planar. The bearing motion is now lagging the shaft centerline disk motion by almost 45 deg!

Figure 14 shows the mode shape and log dec with the damping further increased to 500 lb-sec/in. In this

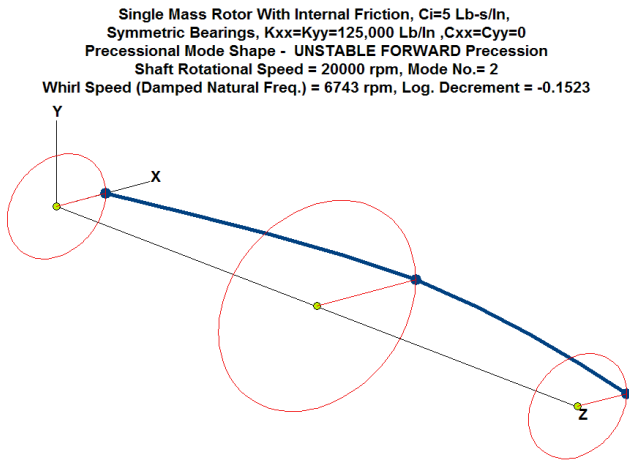


Fig. 12 Unstable Whirl at 20,000 Rpm at Nf = 6,743 CPM With Cb = 0, Log Dec = -0.1523

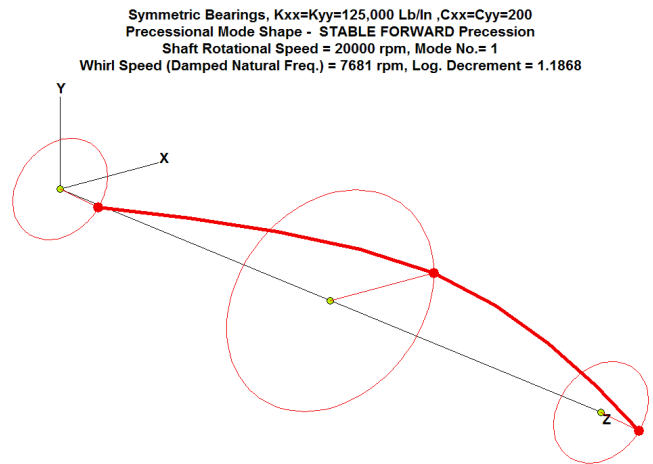


Fig. 13 Stable Whirl at 20,000 Rpm at Nf = 7,681 CPM With Cb = 200, Log Dec = 1.186

case, the log dec has been reduced to -.687 and the whirl frequency has increased to 9,121 CPM. The bearing motion is now lagging the disk motion by about 75 deg. It is obvious that the shaft mode shape is no longer planar. Figure 15 represents the extreme case in which the damping has been increased to the value of Cb=5,000 lb-sec/in. This case represents “*damper lockup*” in which the bearings approach pinned supports and the log dec approaches zero. Any further increase in damping will cause the rotor to go unstable! Hence we see that Eq 8 is only an approximation and accurate only for small bearing lag angles.

There is an important conclusion that can be gained from the behavior of this “simple Jeffcott rotor”. Many large finite element programs and a number of rotor dynamic codes use component modal synthesis for dynamic analysis of aircraft engines and turbochargers with nonlinear bearings. This method is based on planar modes and does not have suitable accuracy to correctly compute highly nonlinear bearings!

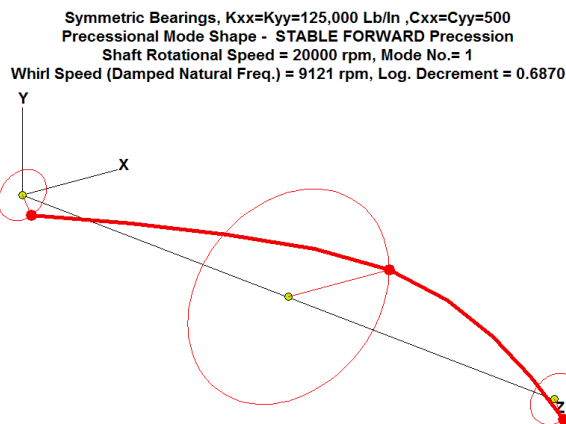


Fig. 14 Stable Whirl at 20,000 Rpm at Nf = 9121 CPM With Cb = 500, Log Dec = 0.687

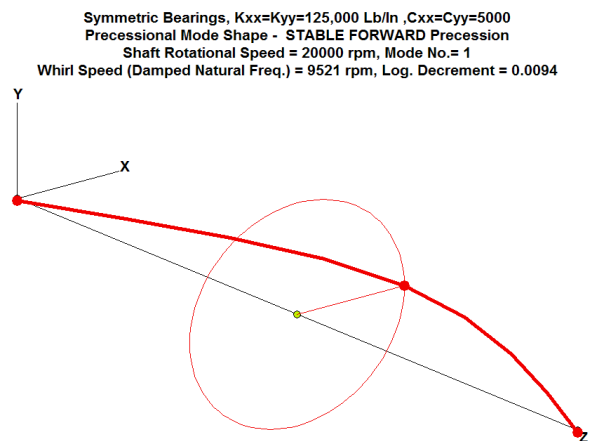


Fig. 15 Stable Whirl at 20,000 Rpm at Nf = 9521 CPM With Cb = 5000, Log Dec = 0.0094

## Stability of Jeffcott Rotor With Internal Friction on Asymmetric Supports

Figure 16 represents the single mass Jeffcott rotor on damped flexible supports (1). The bearing stiffnesses in the horizontal and vertical  $K_x$  and  $K_y$  are identical for both bearings. It is assumed that only cylindrical motion occurs and the operating speeds are well below the conical mode. The equations of motion are represented by 4 degrees of freedom.

If bearing or support mass is included in the model, then the system characteristic equation for stability analysis is 8<sup>th</sup> order. However, if bearing mass is neglected, then the characteristic equation is reduced to a 6<sup>th</sup> order equation. A further reduction in the characteristic equation is achieved assuming low values of internal friction. This reduces the system stability equation to a 4<sup>th</sup> order system.

While this is a reasonable assumption for the study of internal friction on rotor stability, it will be shown that this is not an accurate assumption for the case of aerodynamic cross coupling forces acting on the rotor.

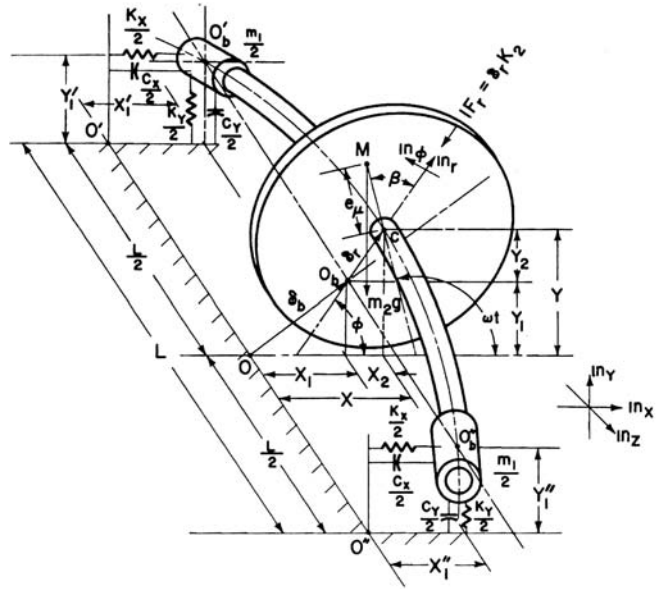


Fig. 16 Jeffcott Rotor on Asymmetric Supports

Figures 17 and 18 represent the relative stability of the Jeffcott rotor for various ratios of vertical flexibility  $R$  as a function of the bearing asymmetry ratio  $\alpha$ . As the vertical support flexibility is increased, the stability is reduced with symmetrical bearings.

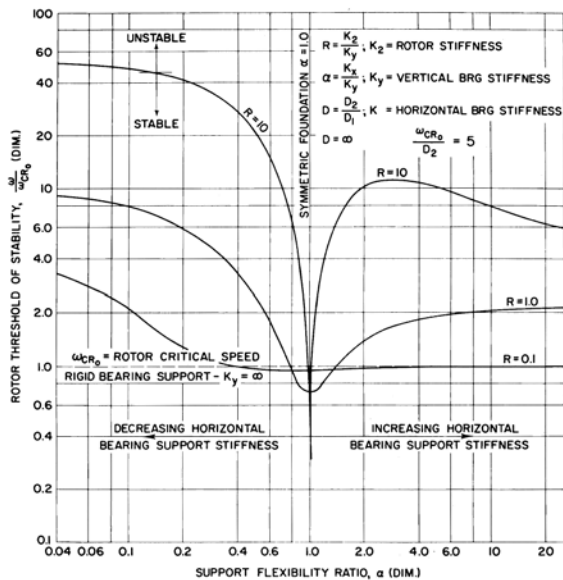


Fig. 17 Rotor Stability With Asymmetric Supports and Zero Bearing Damping

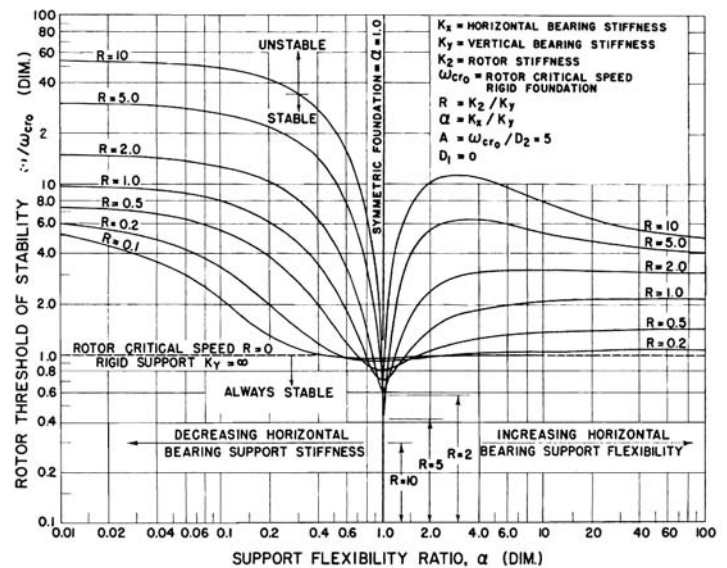


Fig. 18 Stability For Various Values of  $R$  With Asymmetric Supports and Zero Brg Damping

Figure 19 represents a 3 dimensional model of the stability characteristics of the rotor with increasing flexibility  $R$  in the vertical direction for various values of bearing asymmetry  $\alpha = K_x/K_y$ . As shown before, if we simply make a uniform flexible support with no included damping, the system critical speed is reduced along with the rotor stability threshold. Therefore simple support flexibility reduces the stability threshold. Figure 20 shows the important feature that as the value of internal friction increases ( smaller  $A$  values) then *the influence of bearing asymmetry is reduced!*

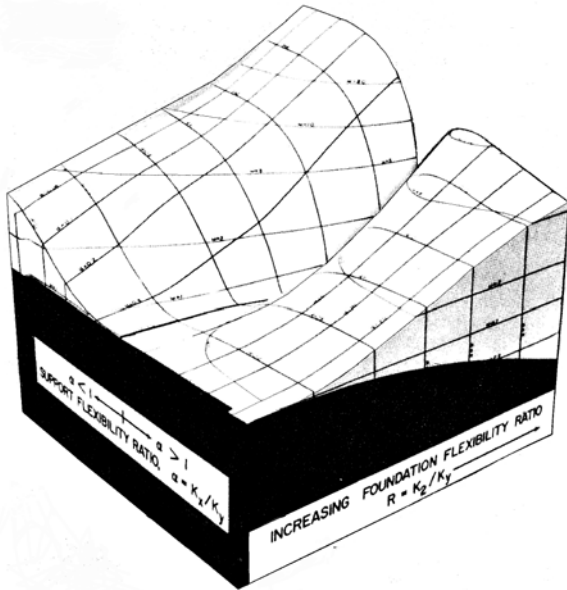


Fig. 19 3 Dimensional Stability Model With Asymmetric Supports and Zero Brg Damping

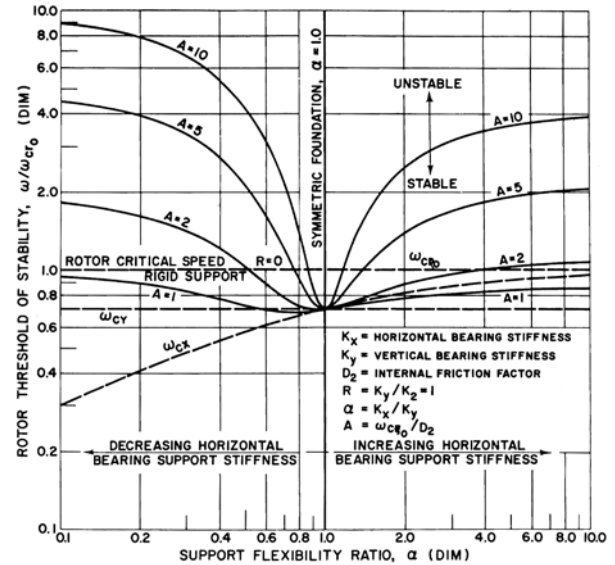


Fig. 20 Influence of Internal Friction Value on Stability For Various Values of  $R$  With Asymmetric Supports and Zero Brg Damping

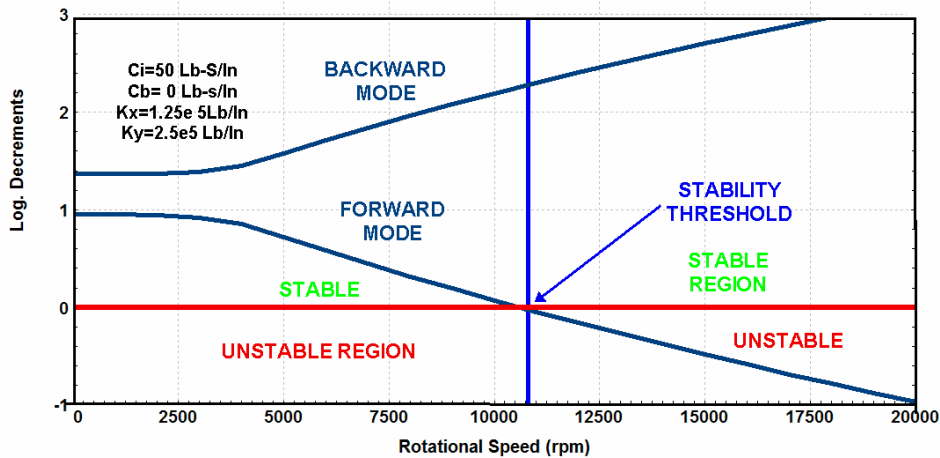


Fig. 21 Stability Plot With Bearing Asymmetry and Zero Bearing Damping

Figure 21 represents a plot of the system log decrement with  $R = K_y/K_x = 2$ ,  $C_i = 50 \text{ lb-s/in}$  and zero bearing damping. In this case, the stability threshold has been increased to over 10,800 RPM. This is a dramatic improvement over the original reduced stability threshold caused by incorporating the symmetric flexible support.

## Discussion of The Influence of Bearing Asymmetry on Rotor Stability Improvement With Internal Friction

When bearing asymmetry is incorporated into the system, then two planar modes are created that are different in the horizontal and vertical directions. Figure 22, for example, represents the horizontal mode corresponding to the horizontal bearing stiffness value of  $1.25 \times 10^6$  lb/in with a natural frequency of 6,753 CPM. Figure 23 represents the vertical natural frequency of 7,715 CPM corresponding to the higher vertical bearing stiffness of  $2.5 \times 10^5$  lb/in.

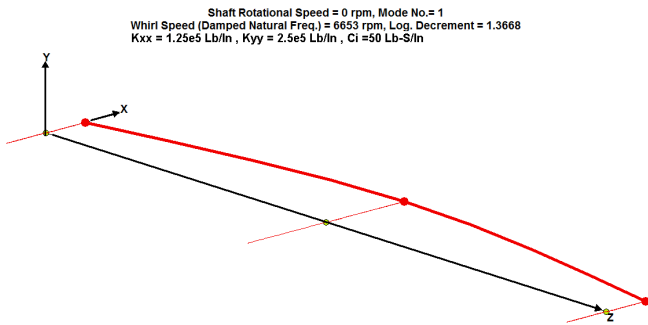


Fig. 22 Horizontal Mode At Zero Rpm  
 $K_{xx} = 1.25 \times 10^6$  Lb/In, 6753 CPM

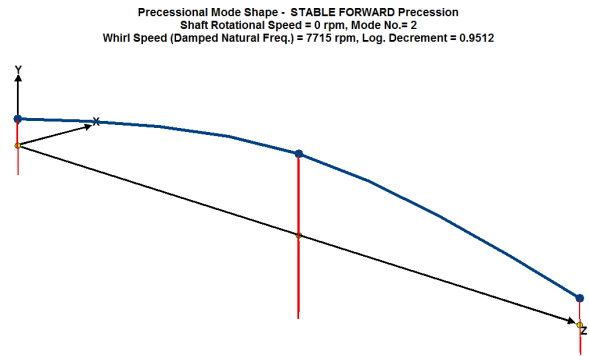


Fig. 23 Vertical Mode At Zero Rpm  
 $K_{yy} = 2.5 \times 10^5$  Lb/In, 7715 CPM

Figure 24 represents the damped mode shape of the rotor at 20,000 RPM with the above specified bearing stiffness coefficients. The rotor is stable with a log decrement of 0.232. This figure should be contrasted to Fig 25 which shows a highly unstable mode at 20,000 RPM. In this case the bearing stiffnesses in both the horizontal and vertical directions are identical.

Dr. Bert Newkirk, in 1924 was not able to explain why this phenomena occurred. In my thesis presentation in 1965, I was unable to articulate exactly why this was possible. However, it was pointed out at that time that the influence of bearing asymmetry was the greatest when the value of internal friction was small. For larger values of internal friction, the influence of bearing asymmetry diminishes rapidly as shown in Fig. 20. The reason for this effect was first explained clearly to me by Dr. Wen Jeng Chen of Eigen Technology. ( It is of interest to note is that all figures presented in this paper use the *DyRoBeS* rotor dynamics software developed by Dr. Chen ). The reason that bearing asymmetry improves stability with internal friction is that it creates elliptical mode shapes as shown in Fig. 24. This minimizes the value of internal friction developed in the rotor. As an example, if the rotor is vibrated in a plane, the internal friction simply acts as conventional damping. In Fig. 25, the mode shape is circular, maximizing the effect of internal friction.

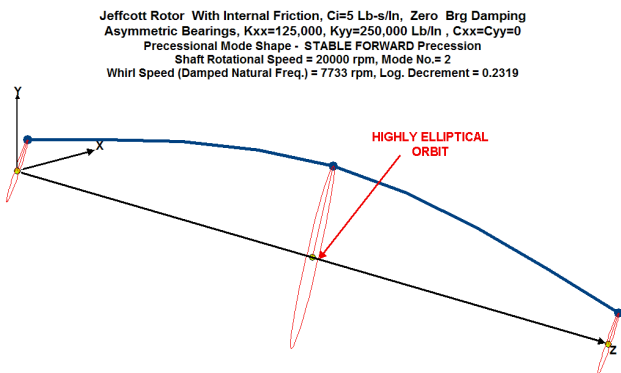


Fig. 24 Stable Mode At 20,000 RPM With Bearing Asymmetry,  $C_i = 5$  Lb-S/In

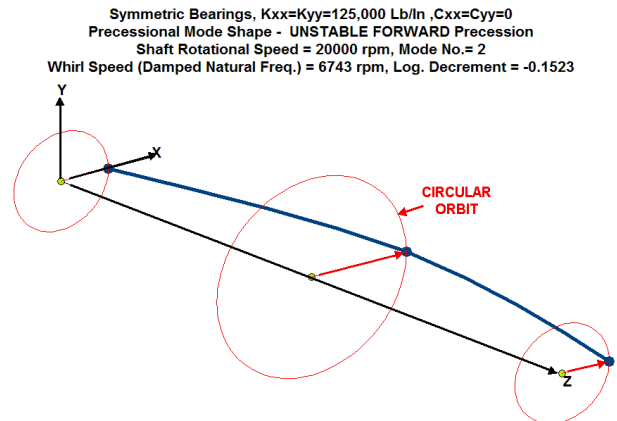


Fig. 25 Unstable Mode At 20,000 RPM With Symmetrical Bearings,  $C_i = 5$  Lb-S/In

## Jeffcott Rotor With Aerodynamic Cross Coupling on Rigid Supports

Another mechanism that can cause self excited whirl motion is referred to as the Alford effect(4). This effect can be generated by aerodynamic forces in both turbines and compressors. This mechanism generates cross coupling terms similar to the cross coupling terms in a fluid film bearing. As Alford first described the effect for turbines, the radial displacement of the turbine wheel causes a local change in the wheel efficiency. This local change in efficiency generates forces to act perpendicular to the deflected centerline of the shaft. For small displacements, this effect may be represented as two similar out of phase bearing forces acting at the disk center. Therefore for the Jeffcott rotor on rigid or stiff supports, the two governing equations of motion would be as follows:

$$\begin{aligned} M\ddot{X} + C_2\dot{X} + KX + QY &= Me_u\omega^2\text{Cos}(\omega t - \phi_u) \\ M\ddot{Y} + C_2\dot{Y} + KY - QX &= Me_u\omega^2\text{Sin}(\omega t - \phi_u) \end{aligned} \quad (9)$$

In the analysis of stability of the Jeffcott rotor under the influence of aerodynamic cross coupling, it will be assumed that there is some positive damping acting at the rotor center. This damping term is shown as  $C_2$ . This small value of damping is assumed to be 5 lb-s/in and will cause an amplification factor of 25 at the critical speed.

Aero Q=10,000 Lb/In, Kbrg=1.0e7 Lb/In - 20 Cycles at Rotor Speed: 20000 rpm  
Station: 2  
X disp: Min = -4.9613, Max = 3.8974  
Y disp: Min = -4.7744, Max = 4.7490

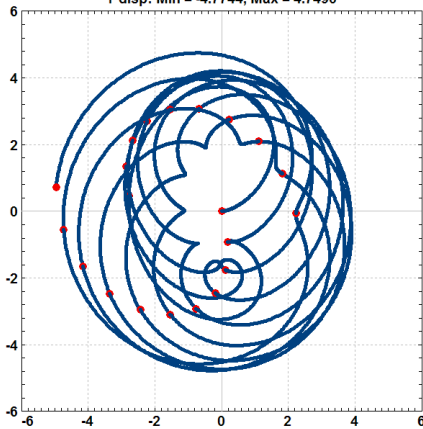


Fig. 26 Whirl Motion With Aerodynamic Q at 20,000 RPM - Stiff Brg Supports

Bearing Forces With Rigid Supports at Rotor Speed: 20000 rpm  
Bearing no.: 1 at Station: 2  
Y force: Min = -27.824, Max = 26.526

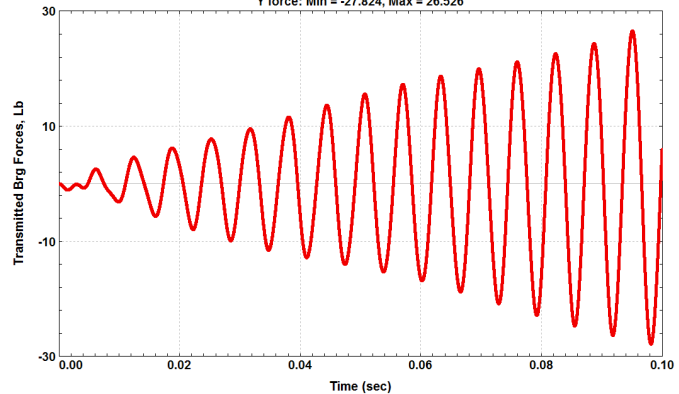


Fig. 27 Bearing Forces With Aero Q at 20,000 RPM Stiff Brg Supports - Kbrg = 1.0e7 Lb/In

Figure 26 represents the whirl orbits of the Jeffcott rotor at 20,000 RPM for 20 cycle of shaft motion with an assume aerodynamic cross coupling value of 10,000 Lb/In and center plane damping of 5 Lb-s/In. In addition, a rotating unbalance of 1.6 oz-in has been added. This value was chosen to displace the rotor center approximately 1 mil. The amplitudes shown if Fig. 26 represent mils of motion. If the rotor were stable, then the orbit radius at this speed above the critical speed would be 1 mil. Since there are no nonlinear shaft forces acting on the rotor, there will be no limit cycle achieved. Hence the motion will continue to increase.

Figure 27 represents the bearing forces transmitted at 20,000 RPM with the assigned aerodynamic cross coupling of 10,000 Lb/In and the stiff bearing support values of 1.0e7 Lb/in. If perfectly rigid bearings are assumed, then the bearing forces can not be computed! It is seen that the bearing forces continue to increase in time and will become unlimited for the assumed linear system. The frequency of the linear growth takes place at the system natural frequency.

## Jeffcott Rotor With Aerodynamic Cross Coupling on Flexible Supports

Figure 28 represents the Jeffcott rotor whirl orbit in which the bearing or support system is reduced in stiffness to a value of  $K_{brg} = 2.5e5$  Lb/In. In this model, the bearing stiffness values are identical in both the horizontal and vertical directions. The reduction in bearing stiffness has caused the rotor orbit to increase greatly over the orbit as shown in Fig. 26. In this model, a small amount of nonlinear shaft stiffness was added to develop a limit cycle of motion.

Figure 29 represents the bearing forces transmitted with the reduced bearing support system. In a linear system, the forces would continue to increase in time as shown in Fig. 27. A small nonlinear shaft stiffness component was added to create limit cycle motion and constrained bearing forces as shown in Fig. 29. Figure 29 shows the bearing forces transmitted vs time. Without the nonlinear shaft stiffness addition, the bearing forces would become unlimited with time. The nonlinear response is apparent after 0.05 seconds of motion. The beating motion occurs due to the interaction of the unbalance with the nonlinear shaft response.

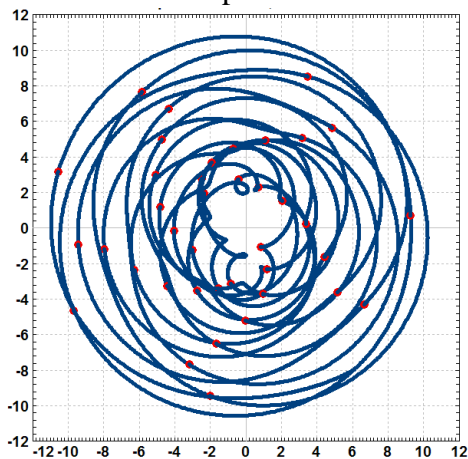


Fig. 28 Whirl With Aero Q at 20,000 RPM,  $-K_{xx}=K_{yy}=2.5e5$  Lb/In

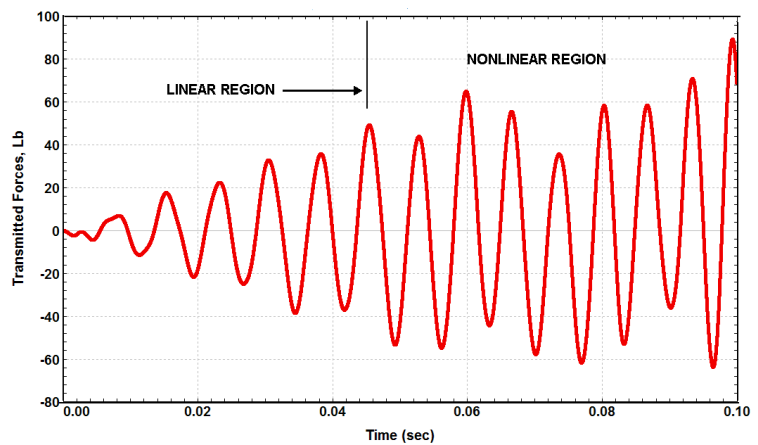


Fig. 29 Bearing Forces With Aero Q at 20,000 RPM With Symmetric Bearing Supports -  $K_{brg} = 2.5e5$  Lb/In

Bearing Forces With  $Q=10,000$  &  $K_{yy}=2.5e5$ ,  $K_{xx}=1.25e5$  Lb/In at Rotor Speed: 20000 rpm  
Bearing no.: 1 at Station: 2  
X force: Min = -65.212, Max = 65.047

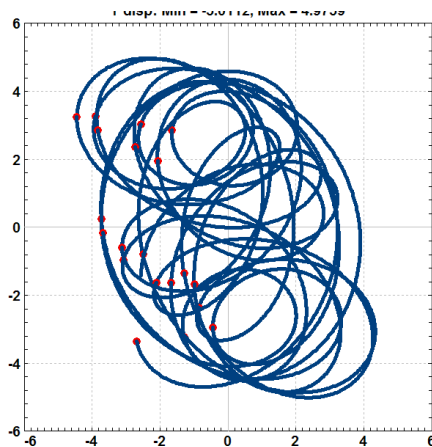


Fig. 30 Whirl With Asymmetric Bearings  $K_{xx} = 1.25e5$ ,  $K_{yy} = 2.5e5$  Lb/In

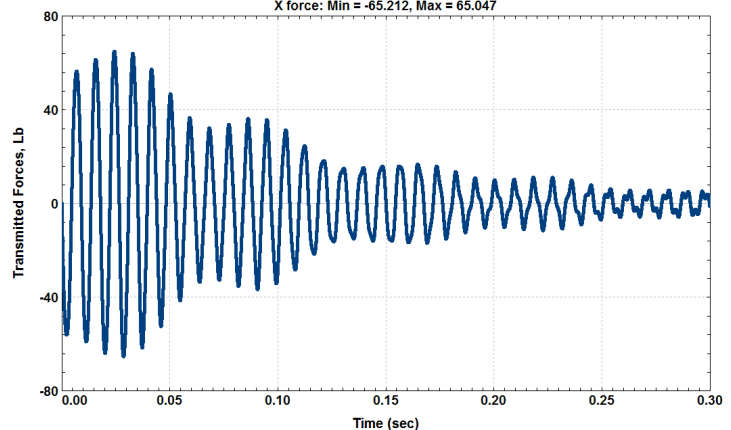


Fig. 31 Bearing Forces With Aero Q at 20,000 RPM With Asymmetric Bearing Supports -  $K_{xx} = 1.25e5$  Lb/In

Figure 30 shows the whirl orbit with the horizontal stiffness reduced in half to  $1.25e5$  Lb/In. The rotor system has been stabilized by the asymmetric support. In Fig. 26, with the symmetric support, the maximum Q value is 8,500 Lb/In. With the asymmetric support, the maximum Q value **has increased by a factor of 4 to 35,000 Lb/In!** Figure 31 shows the bearing forces with the asymmetric support.

## Stability of Multistage Compressors in Tilting Pad Bearings With Aerodynamic Cross Coupling

In the early 1950's, compressor design was limited in speed and number of stages, usually 8 or less. The reason for this was the occurrence of self excited whirling with fixed fluid film bearings. At that stage of development, there did not exist the computer tools for computation of fluid film bearing characteristics, rotor damped eigenvalues (stability) or instrumentation to measure vibrations and determine frequency content. The concept of tilting pad thrust and radial bearings, however, had been in existence for many years. The 5 tilting pad bearing seemed a natural advancement for centrifugal compressor applications because of its superior stability characteristics over fixed plain or elliptic bearings currently in use.

Lund, in 1964 (*who many of us consider to be the father of modern rotor dynamics*), presented his classical paper on "Stiffness and Damping Coefficients for the Tilting Pad Journal Bearing". At that time, however, there did not exist the software to compute rotor stability. It was 10 years later that Lund published his article on rotor stability based on the transfer matrix approach. At this same time, another significant development was the introduction of the Bently noncontact induction probes to monitor vibrations. The ability to perform an FFT analysis of the motion was a later development. Thanks to the cold war, the NAVY spent significant funds on FFT analysis and instrument development. While working on the Space Shuttle engines, I received a major grant from HP for their latest analyzer. It came in three components. The reason was that it have to be able to fit through the front hatch of a nuclear attack submarine!

Compressor design in the 1970's progressed rapidly with designs over 10 stages and speeds in exceeding 10,000 RPM. The instability mechanism that Alford reported in 1965 now began to effect these new high speed, high pressure compressor designs with self excited subsynchronous whirling. A major problem was that this behavior was not detected on the test stands as few full high pressure tests were conducted then. This was a particularly difficult problem when the subject compressor was located on an off shore platform in the North Sea. Many of these compressor problems were corrected by incorporating squeeze film dampers with the tilting pad bearings. We will show that, in many cases, resorting to a squeeze dampers is not necessary. An alternate design using a 4 pad bearing configuration may be sufficient.

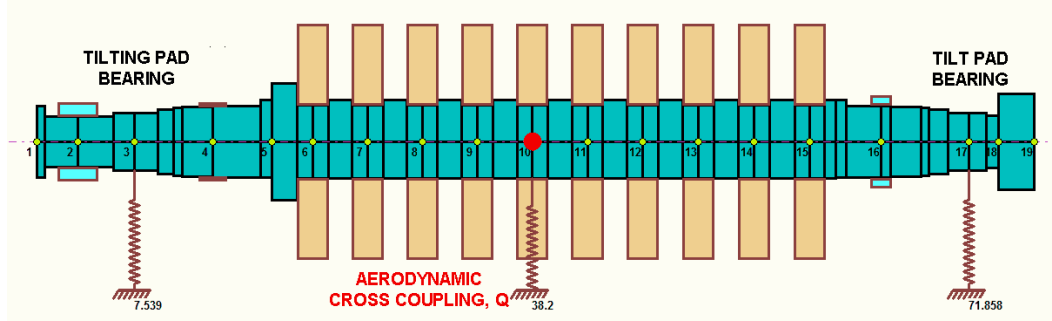


**Fig. 32 Ten Stage Centrifugal Compressor With Tilting Pad Bearings**

Figure 32 represents the 10 stage compressor mounted on 5 pad tilting pad bearings. The 5 pad bearing configuration is very typical for multistage compressors operating above 7,500 RPM. The design is based on the assumption that this bearing will be a superior bearing for resisting instabilities because of its asymmetric bearing coefficients and lack of bearing cross coupling terms (neglecting pad inertia effects). Also shown in the figure is the assumption of the aerodynamic cross coupling as acting at the rotor center. The actual aerodynamic cross coupling coefficients act at all compressor stations. In the following analysis, the total effective  $Q$  will be assumed acting at the rotor center. This has shown to be a reasonable assumption. Figure 32 represents a system with 19 nodes and 76 degrees of freedom. To determine the time transient motion of this system, it will be necessary to integrate the 76 degrees of freedom several hundred times for each cycle of motion. The characteristic equation is of order 152 for damped roots.

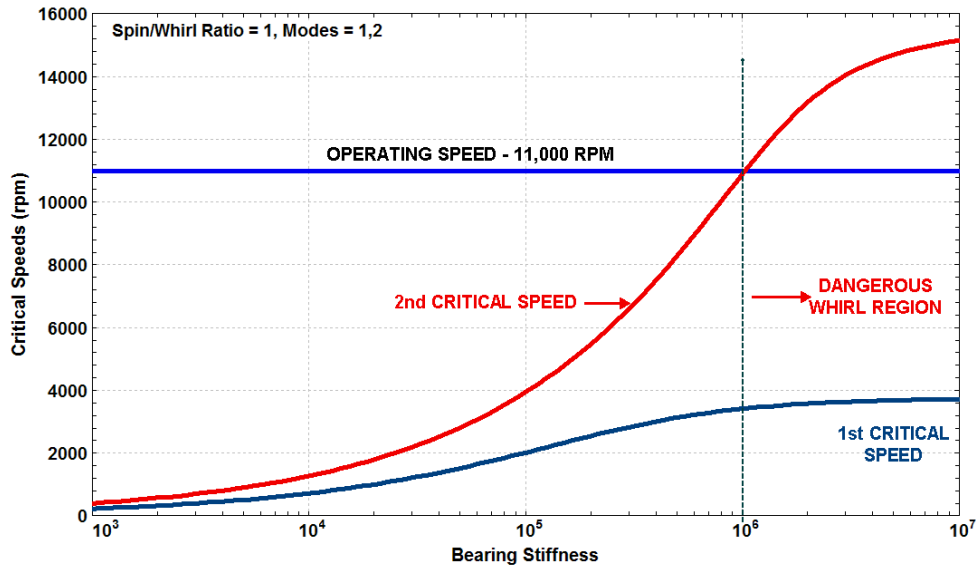


Fig. 33 Critical Speed Map of 10 Stage Compressor

Figure 33 represents the undamped critical speed map of the compressor for various values of bearing stiffness. Reviewing only the undamped critical speed map, for example, can lead to some dangerous conclusions and disastrous designs. For example, viewing the critical speed map, we see that for a nominal bearing stiffness value of  $1.0 \times 10^6$  Lb/In, the compressor will be operating on top of the critical speed. ***This is not a problem!*** A far bigger problem would be to increase the bearing stiffness above  $1.0 \times 10^6$  Lb/In in order to elevate the second critical speed above running speed. This, in effect pinched the bearings, causing small deflections and reducing effective modal damping for the first mode. The rotor system now is highly sensitive to self excited whirl forces. This is a good example of where a little bit of knowledge can be a dangerous thing!

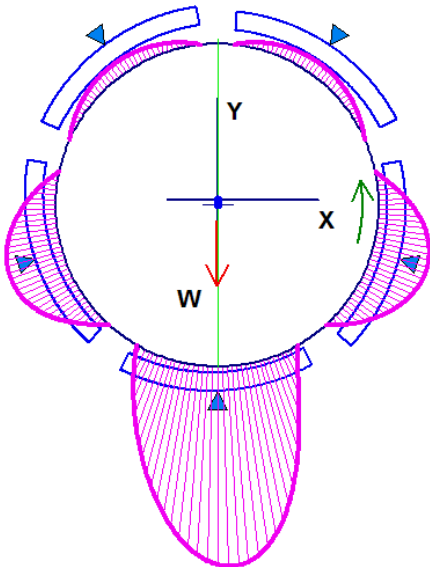


Fig. 34 5 Pad Bearing, Load on Pad  
 $C_b = 5$  Mils,  $Plf=0.5$

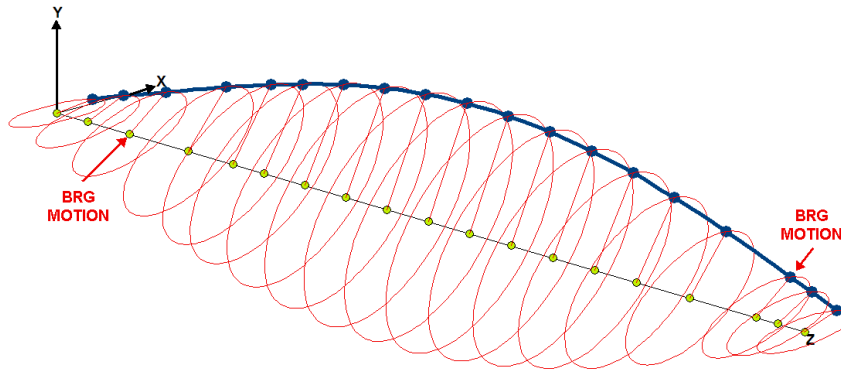
$L/D = 0.6667$ ,  $C_b = 0.006$ ,  $2C_b/D = 0.00267$ ,  
 Speed = 11000 rpm  
 Load = 660 Lbf  
 $W/LD = 48.8889$  psi  
 Vis. =  $1E-06$  Reynolds  
 $S_b = 0.52734$   
 $E/C_b = 0.4807$   
 Att. = 0.00 deg  
 $h_{min} = 2.585$  mils  
 $P_{max} = 217.928$  psi  
 $H_p = 6.92832$  hp  
 $Q_{side} = 5.260$  gpm  
 Stiffness (Lbf/in)  
 1.356E+05 0.000E+00  
 0.000E+00 3.985E+05  
 Damping (Lbf-s/in)  
 1.320E+02 0.000E+00  
 0.000E+00 2.540E+02

Fig. 35 Characteristics of 5 Pad Bearing,  $C_b = 6$  Mils

Figure 34 represents the bearing pressure profile for the 5 pad bearing with load on pad. Figure 35 represents the bearing parameters and shows the stiffness and damping coefficients for the bearing.

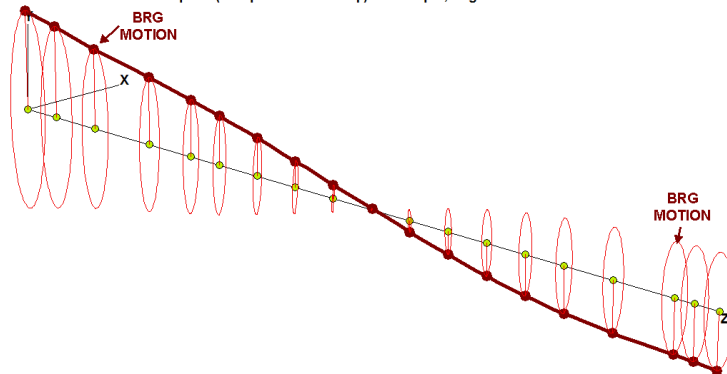
### Stability of 10 Stage Compressor in 5 Pad Bearings With Aerodynamic Cross Coupling - $C_b = 6$ Mills

Figure 36 represents the first forward mode shape (eigenvector) at 11,000 RPM with the specified aerodynamic cross coupling. The whirl frequency is low and is less than  $1/3$  of running speed. The log decrement for this mode is  $-0.99$  which makes this system highly unstable.



**Fig. 36 1<sup>st</sup> Forward Mode With 5 Pad Brg & 6 Mil  $C_b$**

Whirl Speed (Damped Natural Freq.) = 7214 rpm, Log. Decrement = 1.3642



**Fig. 37 2<sup>nd</sup> Forward Mode at 7214 CPM With 5 Pad Brg & 6 Mil  $C_b$  Stable Mode LD = 1.34**

Figure 37 represents the 2nd critical speed. This mode is not of concern and will not be excited by unbalance since the log decrement is 1.34. The large amplitude at the bearings creates significant damping. Figure 38 shows the 3<sup>rd</sup> mode near running speed at 11,078 RPM. This is not a problem for unbalance response.

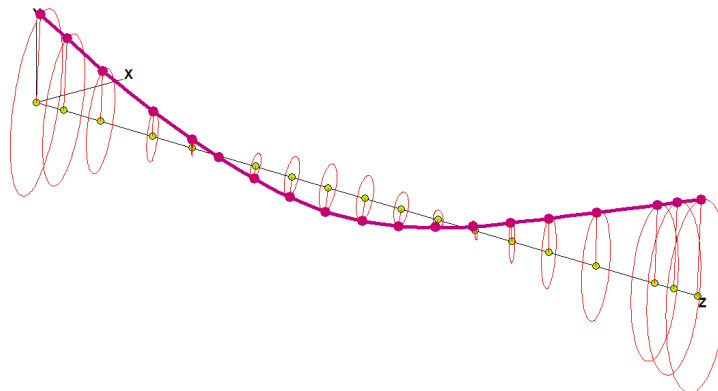


**Fig. 38 3<sup>rd</sup> Forward Mode at 11078 CPM With 5 Pad Brg & 6 Mil  $C_b$  Stable Mode Log Dec = 1.26**

**Stability of 10 Stage Compressor in 5 Pad Bearings With Aerodynamic Cross Coupling -  $C_b = 4$  Mils**

In an attempt to improve stability, the bearing clearance has been reduced from 6 mils to 4 mils. Figure 39 shows the resulting bearing pressure as a result of the reduced bearing clearance. Figure 40 represents the bearing parameters and bearing coefficients generated by the reduction in bearing clearance. The stiffness in the x direction has almost tripled while the vertical stiffness has increased by 40%. Similar increases in damping are also observed.

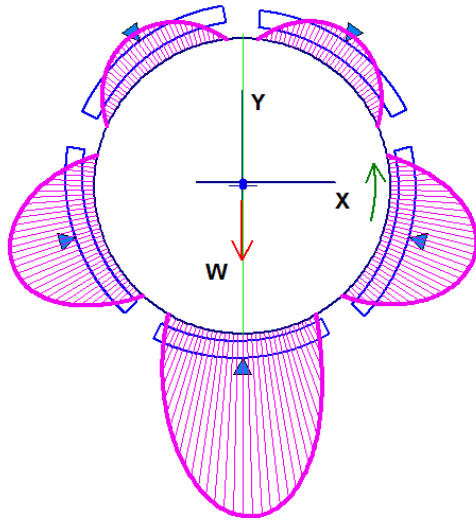


**Fig. 39 5 Pad Brg With Load on Pad ,  $C_b = 4$  Mils  $L/D = 0.666$ , Preload = 0.5**

$L/D = 0.6667$ ,  $C_b = 0.004$ ,  $2C_b/D = 0.00178$ ,  
 Speed = 11000 rpm  
 Load = 660 Lbf  
 $W/LD = 48.8889$  psi  
 Vis. =  $1E-06$  Reynolds  
 $S_b = 1.1865$   
 $E/C_b = 0.2936$   
 Att. = 0.00 deg  
 $h_{min} = 2.414$  mils  
 $P_{max} = 229.12$  psi  
 $H_p = 9.47685$  hp  
 $Q_{side} = 3.644$  gpm  
**Stiffness (Lbf/in)**  
 3.812E+05 0.000E+00  
 0.000E+00 5.697E+05  
**Damping (Lbf-s/in)**  
 3.998E+02 0.000E+00  
 0.000E+00 4.999E+02

**Fig. 40 Characteristics of 5 Pad Brg With  $C_b = 4$  Mils  $L/D = 0.666$   $Plf = 0.5$**

10 STAGE CENTRIFUGAL COMPRESSOR,  $N = 11,000$  RPM,  $W = 1,327$  LB,  $C_b = 4$  Mils  
 5 PAD BRGS,  $L/D = 0.666$ ,  $K_{xx} = 381,000$ ,  $K_{yy} = 570,000$  Lb/in,  $C_{xx} = 400$ ,  $C_{yy} = 500$  Lb-s/in  
 AERODYNAMIC CROSS COUPLING  $Q = 50,000$  LB/IN,  $U_b = 2$  Oz-in  
 Precessional Mode Shape - UNSTABLE FORWARD Precession  
 Shaft Rotational Speed = 11000 rpm, Mode No. = 2  
 Whirl Speed (Damped Natural Freq.) = 3230 rpm, Log. Decrement = -0.3065

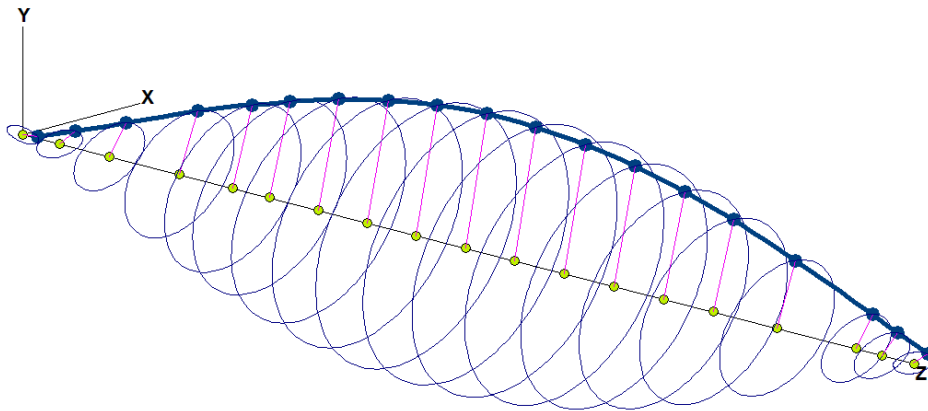


**Fig. 41 Compressor 1<sup>st</sup> Forward Mode With Reduced Clearance 5 Pad Bearing  
 $L/D = 0.666$ ,  $PLF = 0.5$ ,  $m = 0.5$ ,  $Q = 50,000$  Lb/In, Log Dec = -0.303**

Figure 41 represents the first damped forward mode with the tighter clearance 5 pad bearing. With an applied aerodynamic cross coupling of  $Q = 50,000$  Lb/ In, the mode is highly unstable with a log decrement of -0.30. Note that the motion with the stiffer bearing is now more symmetrical. The increased stiffness has also increased the whirl to 3,230 CPM.

### Stabilization of a 10 Stage Compressor With a 4 Pad Bearing Design

Once the aerodynamic cross coupling exceeds approximately a Q value of 20,000 Lb/in, it is difficult to stabilize the system with a 5 pad bearing regardless of clearance values and preloads. The bearing stiffness and damping values are not independent. Thus to stabilize this class of compressor, it has been necessary to resort to mounting the 5 pad bearings in squeeze film dampers. This becomes a complicated design and also may not be adequate for compressors exceeding 10 stages.

For example, one design the author worked on at Fort McMurry (tar sand region of Canada) was an **unstable compressor with 5 pad bearings and squeeze film dampers!** The system was still unstable. The final solution required redesigning 2 internal seals as squeeze film dampers (subject for a future paper). A later review of this compressor using modern analysis techniques showed that this 8 stage rotor could easily have been stabilized by the proper design of 4 pad bearings. However, at that time we did not know what the proper tilting pad bearing coefficients that should be designed for. At that time and also currently today, the 5 pad bearing configuration appears to be the preferred approach by the various manufactures. This design approach has been a bonanza for the consultants over the last several decades for correcting stability problems.

#### Shaft Modal Stiffness, $K_{shaft}$

Before we can properly design a tilting pad bearing for the multistage compressor, it is first necessary to determine a fundamental property of the system. Without the knowledge of this one parameter, we could endlessly be computing various 5 or 4 pad bearings without arriving at a satisfactory bearing design. The basic parameter that is required in order to properly design an effective 4 pad bearing is the knowledge of the shaft modal stiffness. This value can be computed from the critical speed analysis. The modal mass corresponding to the rigid support critical speed is computed. If this value is not available, then a value of 55% of the total rotor weight is of sufficient accuracy. Note that the modal weight of a uniform shaft is exactly  $\frac{1}{2}$  the shaft weight.

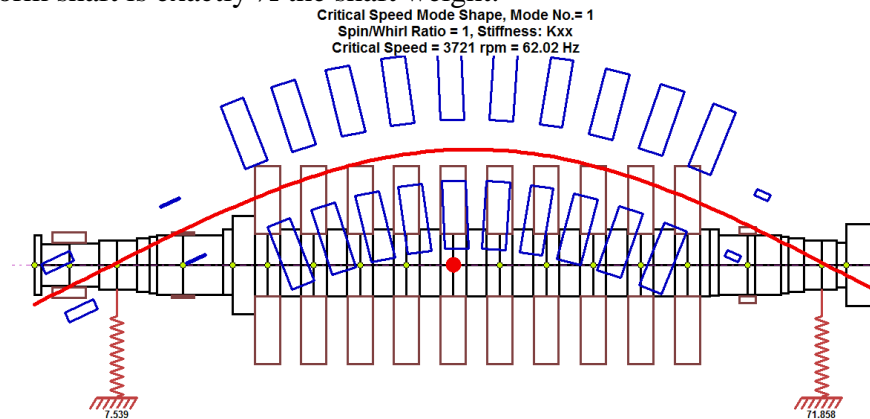


Fig. 42 Compressor Critical Speed on Rigid Supports

$N_{cr} = 3,271 \text{ RPM}$

Figure 42 represents the compressor critical speed on rigid supports. This frequency is computed at 3,271 RPM. Note that this value could also have been obtained from the critical speed map as shown in Fig.33. The modal weight was computed as 710 Lb which is 54% of the total rotor weight. The fundamental shaft stiffness may now be computed as follows:

$$K_{shaft} = \frac{W_{modal}}{g} \times \left( \frac{N_{cr} \cdot 2\pi}{60} \right)^2 = \frac{710 \text{ Lb}}{386 \text{ in/sec}^2} \times \left( \frac{3271 \times 2\pi}{60} \right)^2 = 280,000 \text{ Lb / In} \quad (10)$$

### Design Parameter for 4 Pad Bearing

We have essentially reduced the 10 stage compressor to a Jeffcott rotor! The optimum bearing to shaft stiffness ratio has been shown to  $R_{\text{optimum}} = 2K_{\text{brg}}/K_{\text{shaft}} = 1$ . This design parameter is next to impossible to achieve with a 5 pad bearing with load on pad. For example, with Fig. 39 with the 5 pad bearing and load on pad, the R ratio is 2.7. Thus when the values of R exceed unity, there is no amount of bearing damping that will make a highly stable bearing configuration.

With this bearing to shaft stiffness parameter in mind, we now have a design goal to attempt to achieve. As previously mentioned, it will not be possible to design any 5 pad bearing to meet these guidelines. With this in mind, we now examine the 4 pad bearing. What we find out that the 4 pad bearing initially does little to improve the stability. The stiffness is still too high with the l/d ratio of 0.666. We now have the paradox that to improve stability, *we actually have to use a larger bearing with less preload!*

Figure 43 represents a 4 pad load between pad bearing design with an enlarged L/D ratio to 1 and a preload reduced to  $m=0.2$ . These changes are, at first, counter intuitive. The reason for the larger clearance is to “float the shaft” in order to obtain a lower bearing stiffness.

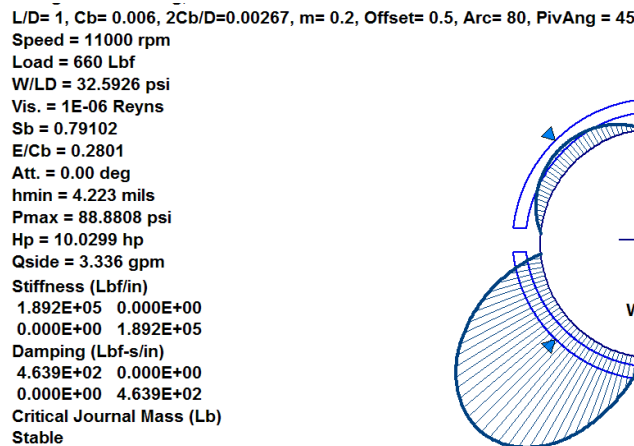


Fig. 43 4 Pad Bearing With L/D=1.0, Preload = 0.2, Cb = 6 Mils

The R ratio for this design is 1.35 which is close to optimum. If the shorter L/D ratio is used, than the R ratio will be over 2. Thus we are using a larger bearing, not for increased load capacity, but to obtain a softer bearing support. Fig. 44 shows a stable whirl mode with the enlarged 4 pad bearing.

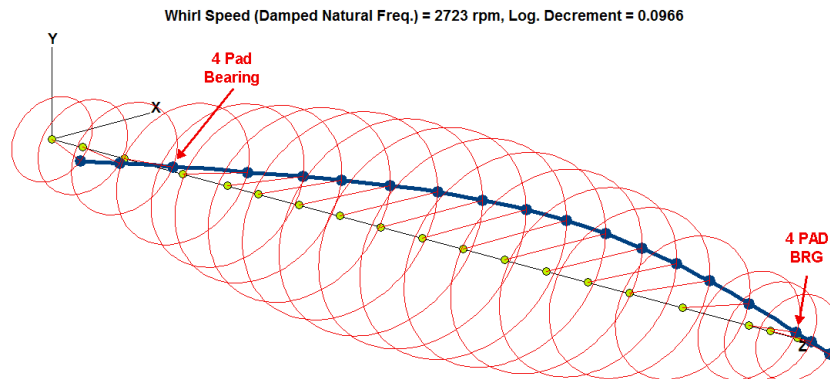


Fig. 44 Stable Mode at Threshold of Stability With 4 Pad Brg  
L/D =1, Cb=6 Mils, Q=60,000 Lb/In, Log Dec =0.096

## Time Transient Behavior With 5 and 4 Pad Bearing Configurations

Time transient analysis was performed on both the 5 and 4 pad bearing designs to show the difference in amplitudes of motion and bearing forces transmitted. In both cases, aerodynamic cross coupling of  $Q=50,000$  Lb/In is included at the mass center as well as an unbalance of 2 oz-in. The rotor system has a total of 76 degrees of freedom. The motion is evaluated over 10 cycles of motion. A time step of  $1.0e-6$  sec was used which requires over 5,000 time steps for each cycle of motion for each degree of freedom.

Figure 45 shows the unstable transient motion of the rotor with the 5 pad bearings. Figure 46 shows the motion at the rotor center for 20 cycles of motion. The rotor develops large amplitudes of whirl.

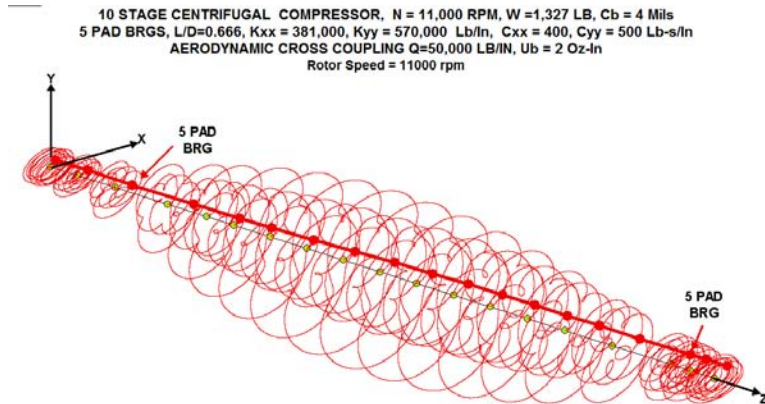


Fig. 45 Transient Motion With 5 Pad Brg & Unbalance

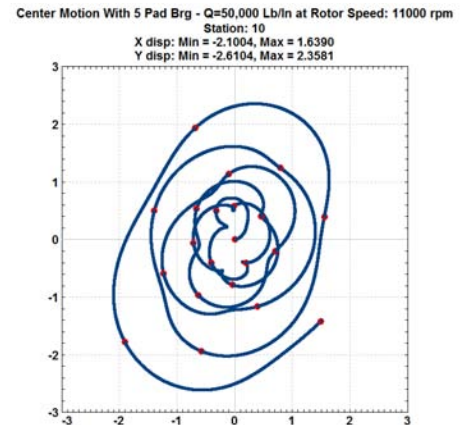


Fig 46 Center Span Motion With 5 Pad Brg For 20 Cycles, Mils

Fig. 47 shows the whirl motion at the 5 pad bearing. Although the initial amplitude is small, it continues to grow. Shown on both Figures 46 and 47 are timing marks to represent each shaft rotation. If the motion was totally synchronous, then the timing marks would align.

Of great importance are the large forces over 400 Lb developed after 20 cycles of motion as shown in Figure 48. The influence of unbalance represents a synchronous response, but is overwhelmed by the large forces generated due to the occurrence of self excited whirling.

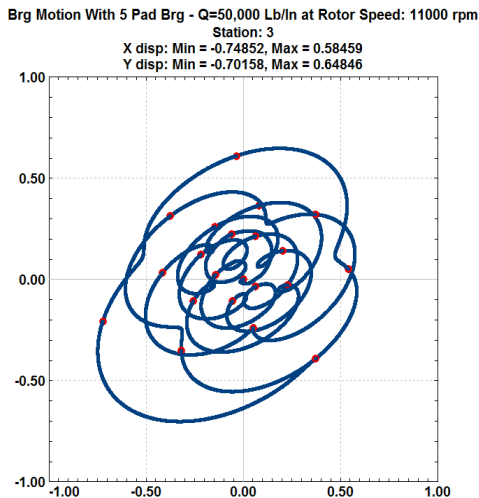


Fig. 47 Bearing Motion With 5 Pad Brg For 20 Cycles, Mils

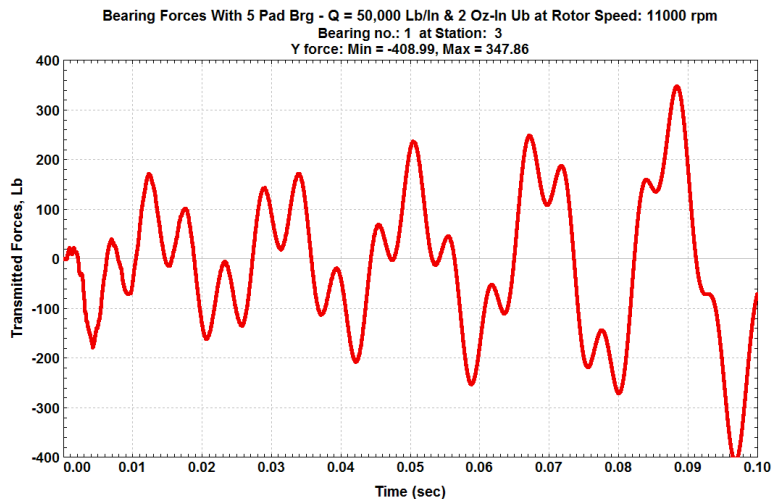
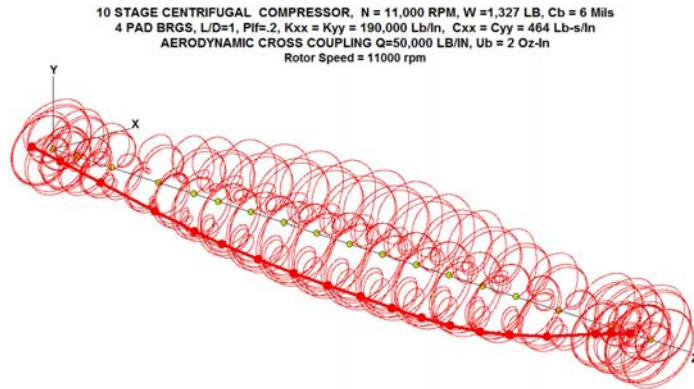
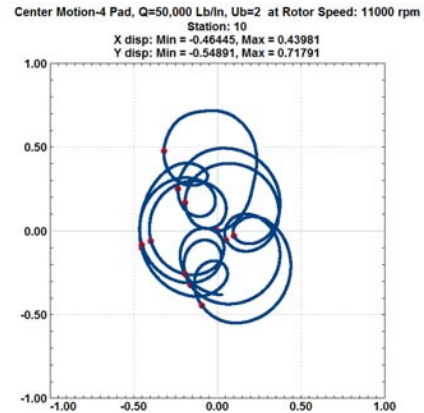


Fig. 48 Bearing Forces With 5 Pad Brg For 20 Cycles

Figure 49 shows the time transient motion with the 4 pad bearing configuration for 20 cycles of shaft motion. The initial transient motion is caused by the excitation of the first forward mode caused by unbalance. After about 5 cycles of motion, the initial transient begins to die out, since this is a stable system. Figure 50 shows the initial motion at the shaft center. The initial maximum excursion is only 0.7 mils caused by the application of the 2 oz-in of unbalance placed at the rotor center.



**Fig. 49 Transient Motion With 4 Pad Brg & Unbalance**



**Fig. 50 Center Span Motion With 4 Pad Brg For 20 Cycles, Mils**

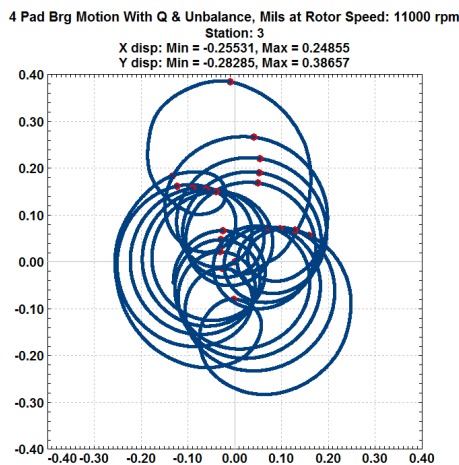


**Fig. 51 Bearing Motion With 4 Pad Brg For 20 Cycles, Mils**

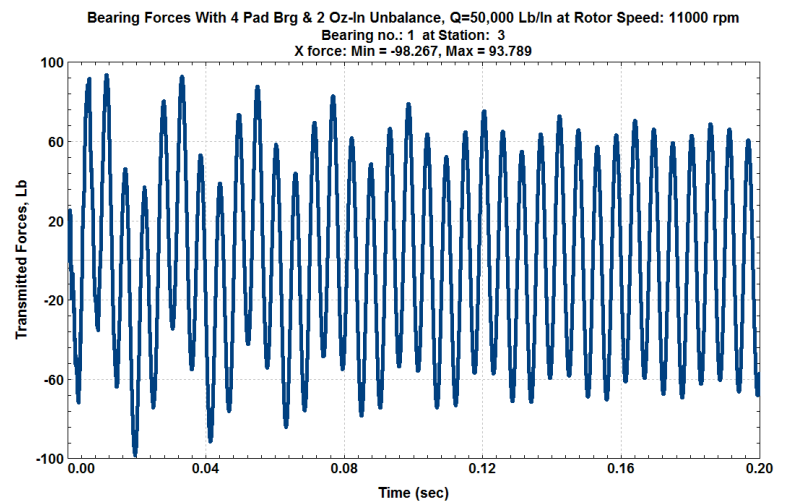


**Fig. 52 Bearing Forces With 5 Pad Brg For 37 Cycles, Lbs**

Figure 51 shows the orbital motion at the bearing location for the case of the 4 pad bearing. We can clearly see the transient motion diminishing after only 5 cycles of motion. If we were to continue the transient calculations for another 20 cycles of motion, we would have only synchronous circular motion caused by the applied unbalance.

Figure 52 shows the bearing forces transmitted over 37 cycles of motion for a time period of 0.2 seconds. The initial oscillations in the bearing forces transmitted is caused by the excitation of the first critical speed. After about 20 cycles of motion, the forces transmitted are predominately synchronous forces caused by the rotating unbalance of 2 oz-in. At this speed, the 2 oz-in of unbalance generates a rotating force of over 470 Lbs. Note that the steady state forces reduce to +1 60 Lbs at each bearing. This case shows the dramatic improvement of the rotor response with 4 pads as compared to the 5 pad design.

## Industrial Application - Kabob of Alberta

The Kabob case history is a perfect example of fractional frequency whirl occurring in a high pressure compressor. The Kabob whirl problem was first encountered in 1971 and the history and design changes were presented in some details at the Fourth Annual Texas Turbomachinery Conference in 1976. This case was of particular interest as two of the references for the motivation for the bearing redesigns were based on several of my publications on the influence of bearing asymmetry on stability with internal friction.

The original Kabob rotor is shown in Fig. 53. The bearing span for this system is shown in the figure as 59.68 inches. Compare this design with the 10 stage compressor as shown in Fig. 32 which has a bearing span of 64.3 inches. It was reported that in order to have a rotor with controlled whirl motion, that a final rotor design was required with a reduced length of 53.43 inches and increased shaft diameter. Based on modern rotor-bearing dynamical analysis, this compressor could have been stabilized by either a properly designed 4 pad bearing or with a squeeze film damper and the 5 pad bearing configuration.

However, attempting to stabilize this rotor using the asymmetrical properties of a 5 pad bearing will not work with the original bearing aspect ratio. Proper bearing design could have saved a reported loss of \$25 million (in 1971 dollars!). Although Lund had earlier presented a major paper on the 5 pad bearing, his paper on rotor-bearing stability was not presented until 1974. Therefore, the major compressor manufacturers did not have the computer tools for extensive rotor-bearing stability studies. Kabob has demonstrated that trial and error bearing replacements can be very expensive.

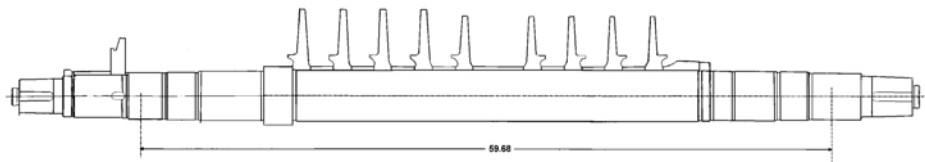


Fig. 53 Original Kabob 9 Stage Compressor Design

## Redesigned 5 Pad Bearing For Exaggerated Bearing Asymmetry

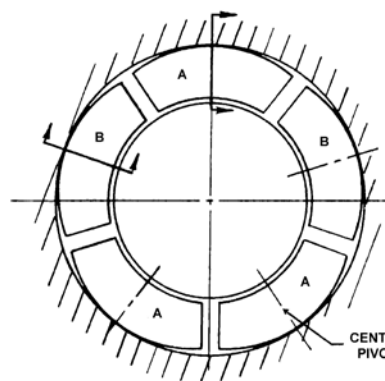
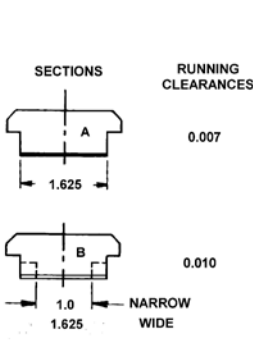


Fig. 54 Redesigned Kabob 5 Pad Brg to Increase Bearing Asymmetry



5 Pad, Load Between Pads Kabob  
 $L/D = 0.4063$ ,  $C_b = 0.007$ ,  $2C_b/D = 0.0035$ ,  $m = 0.2$ ,  $Offset = 0.5$ ,  $Arc = 62$ ,  $PivAng = 18$   
 Speed = 11000 rpm  
 Load = 600 Lbf  
 $W/LD = 92.3077$  psi  
 $Vis. = 1E-06$  Reyns  
 $S_b = 0.16213$   
 $E/C_b = 0.8554$   
 $Att. = 0.00$  deg  
 $h_{min} = 1.714$  mils  
 $P_{max} = 283.947$  psi  
 $H_p = 3.51711$  hp  
 $Q_{side} = 1.362$  gpm  
 Stiffness (Lbf/in)  
 2.316E+05 0.000E+00  
 0.000E+00 4.383E+05  
 Damping (Lbf-s/in)  
 1.216E+02 0.000E+00  
 0.000E+00 2.185E+02  
 Critical Journal Mass (Lb)  
 Stable

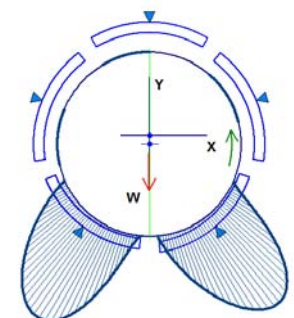


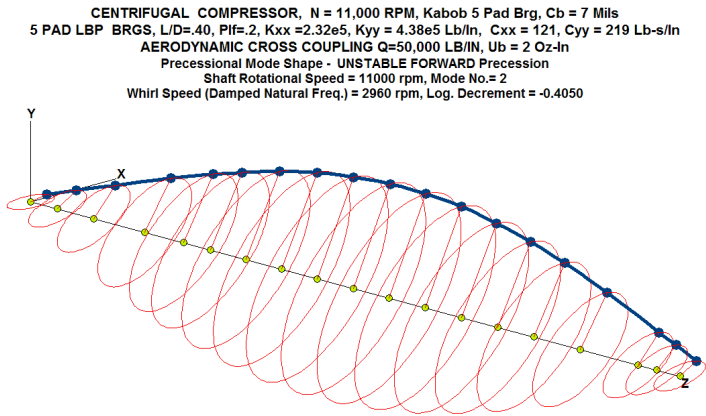
Fig. 55 Computed Brg Coefficients For Redesigned 5 Pad Bearing

Figure 54 shows the redesigned 5 pad bearing to increase the apparent amount of bearing asymmetry. Note that the side pads, labeled B, have a reduced bearing width from 1.625 to 1.00 inches. Also the bearing pad clearance has been increased from 7 mils to 10 mils. Figure 55 shows a computer simulation of the bearing redesign with variable pad length and pad clearance values.

Note that the stiffness and damping values are almost twice as high in the vertical direction as the horizontal direction. The upper 3 pads contribute very little to the overall stiffness and damping values for this bearing.

**Compressor Stability With Redesigned 5 Pad Bearings**

The compressor critical speed on rigid supports for the original rotor design was given as 3,915 RPM. Although the modal mass of the unit was not specified, we can estimate the effective modal shaft stiffness to be of the order of 250,000 Lb/In. From Fig. 55, we see that the vertical bearing stiffness  $K_{yy}$  is 438,000 Lb/In. This places the critical bearing to shaft  $R$  ratio ( $2K_{yy}/K_s$ ) to be over 3! Therefore, we can not expect this bearing design to be effective in rotor stabilization. Figure 56 shows the computed stability corresponding to the bearing coefficients as give in Fig. 55 and a representative rotor model. The log decrement of -0.405 indicates that this bearing design will be highly unstable.



**Fig. 56 Computed 1<sup>st</sup> Forward Whirl Mode For 9 Stage Kabob Rotor in 5 Pad Bearings - Unstable Mode**

**Six Pad Narrow Bearing Design With Included Squeeze Film Damper**

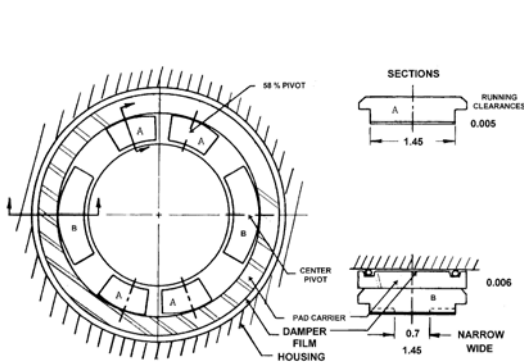


**Fig. 57 Narrow 6 Pad Bearing in 6 Mil Squeeze Film Damper**

L/D= 0.4063, Cb= 0.007, 2Cb/D=0.0035, m= 0.2, Offset= 0.5, Arc= 31, PivAng= 0  
 Speed = 11000 rpm  
 Load = 600 Lbf  
 W/LD = 92.3077 psi  
 Vis. = 1E-06 Reyns  
 Sb = 0.16213  
 E/Cb = 0.9409  
 Att. = 0.00 deg  
 hmin = 1.124 mils  
 Pmax = 441.907 psi  
 Hp = 2.83091 hp  
 Qside = 0.511 gpm  
 Stiffness (Lbf/in)  
 2.897E+05 0.000E+00  
 0.000E+00 8.648E+05  
 Damping (Lbf-s/in)  
 1.147E+02 0.000E+00  
 0.000E+00 3.309E+02  
 Critical Journal Mass (Lb)  
 Stable

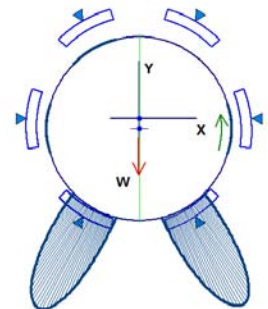


**Fig. 58 Pressure Profile & Brg Coefficients For Narrow 6 Pad Bearing**

Figure 57 shows a 6 pad bearing design with narrow pads. This bearing has an  $R$  ratio of 2.6 which is not a major improvement over the original design. The bearing was mounted in a squeeze film damper. ***This damper is flawed as it does not have a central groove!*** This caused the damper to act as a long bearing damper. The central groove makes a short bearing damper with adequate damping values. A much larger clearance must be used with the long bearing damper. The final design error was to decrease the clearance for the long bearing damper. Thus this damper was ineffective. All of these problems required a redesigned shorter and stiffer shaft. Proper bearing design could have avoided this.

## Industrial Application - 11 Stage Compressor in 5 Pad Bearings

Figure 59 shows an 11 stage compressor that initially encountered a severe whirl problem at full load conditions. At the time this rotor was analyzed, both finite element bearing and stability programs (based on the Lund transfer matrix method) were available for detailed stability analysis. The system was analyzed for various conditions of bearing preload and conditions of load on pad and between pad loading conditions for a 5 pad bearing.

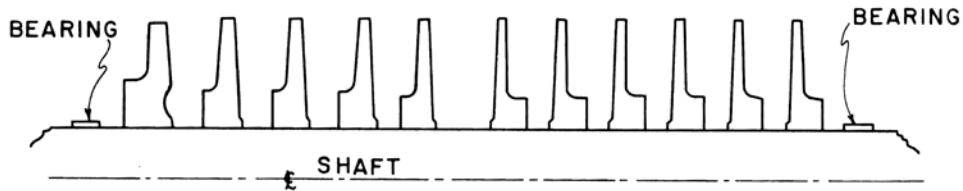


Fig. 59 11 Stage Compressor in 5 Pad Bearings Bearing Span = 70 In, Shaft D = 6 In  
(Nicholas, Gunter, Barrett, 1978)

The 11 stage compressor has a bearing span of 70 inches. The nominal shaft diameter is 6 inches. The computed effective shaft stiffness is  $K_{\text{shaft}} = 280,000 \text{ Lb/In}$ . Figure 60 shows the relative stability of the 11 stage compressor for a variety of loading conditions with the 5 pad bearings. The highest stability is achieved by bearing types 1 and 6. Bearing no. 1 is a load on pad design while bearing no. 6 is a load between pads configuration. In both of these cases, the bearings have zero preload. The zero preload condition leads to softer vertical stiffness values. The worst two bearing designs are similar to bearings 1 and 6 except that the bearing preload has been increased to 0.5! This causes a large increase in the vertical bearing stiffnesses causing a substantial reduction in stability.

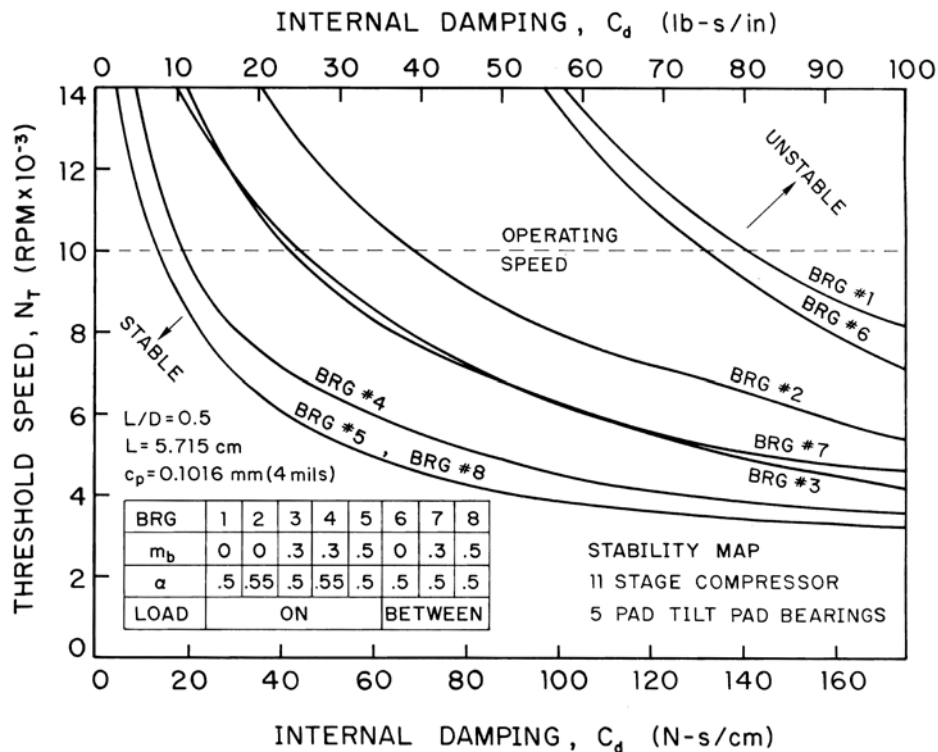
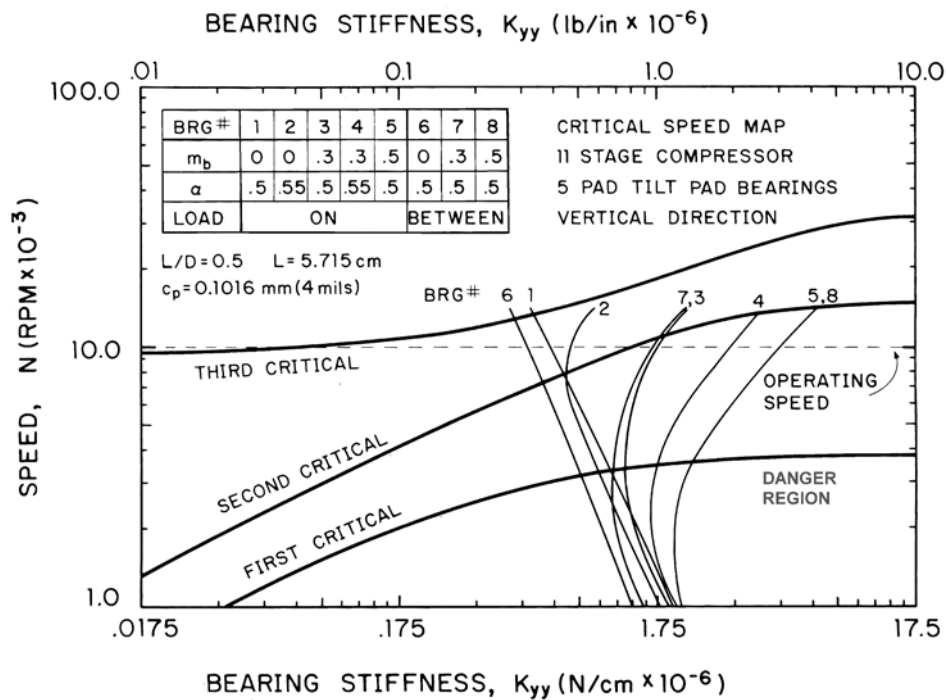


Fig. 60 Stability Map for 11 Stage Compressor in 5 Pad Bearings  
For Various Values of Preload and Load On and Between Pads

Bearing number 1, which is a load between pad design, has a zero preload. This bearing has a vertical stiffness ratio of  $2K_{yy}/K_{\text{shaft}}$  of 2.79. The optimum value is 1. The bearing number 6 is also a zero

preload design with load on pad design. The R ratio for this design is slightly higher at 3.50. These two designs represent the best of the ones analyzed. The worst designs are bearings 5 and 8 which are also load between and load on pad designs, but with the bearing preload increased to 0.5 in both cases. This greatly increases the bearing vertical stiffness values.

These two designs have R ratios of 13.4 and 21. These designs both will allow violent self excited whirl instability to occur. Bearing no. 4 is also very poor in spite of the lower preload value of 0.3. The reason for this is that the design uses an offset pivot of 55% of arc length. This generates greater hydrodynamic bearing pressures and hence excessive bearing stiffnesses. Increasing bearing preload or offset ratio in an attempt to raise stability by increasing bearing stiffness and damping can cause catastrophic failure to occur when the value of twice the vertical bearing stiffness exceeds an order of magnitude above the shaft stiffness. At high R values, bearing asymmetry is of no benefit in stability improvement.



**Fig. 61 Critical Speed Map for 11 Stage Compressor on 5 Pad Bearings For Various Values of Preload and Load On and Between Pads**

Figure 61 shows the critical speed map for the compressor for the various bearing configurations. Bearing types 5 and 8 are often chosen based on the consideration that the compressor will be operating below the second critical speed. This type of design consideration, based on API recommendations, is a recipe for a disaster. It is of interest to note that bearings no. 1 and 6 show that the vertical bearing stiffness values actually decrease with speed. This is due to the zero preload case in which the top pad is not adding additional loading.

As the shaft raises in the bearing with speed, the bearing stiffness becomes softer. Compare this behavior with the preloaded bearings. At speeds above 4,000 RPM, the preloaded top pad can cause a dramatic increase in the net vertical stiffness values. Hence as speed increases, these bearing designs become more sensitive to self excited whirl forces. This dangerous condition can be observed from the critical speed map. If the bearing stiffness at running speed projects down into the indicated danger region, then this bearing type must be redesigned with either a lower preload or a wider 4 pad design.

## Discussion and Conclusions

The use of the 5 pad tilting pad bearing configuration with centrifugal compressors has greatly improved the operating speed range of these machines. This has led marketing departments to propose compressor designs with speeds in excess of 10,000 RPM and compressors with as many as 11 stages. The use of the 5 pad bearing has been particularly popular with manufacturers since this bearing design is not susceptible to self excited hydrodynamic bearing effects.

However, with the increase in speed, number of stages and higher discharge pressures, these machines have become highly sensitive to Alford type of self excited forces generated internally. Under normal low pressure factory testing, this sensitivity condition usually goes undetected and does not appear until the unit is installed and operated under full load conditions.

Vibration monitoring probes are usually placed vertically at the bearing locations. Probes are never placed at the compressor center span for motion detection because of the difficulties involved. The safety of the unit is usually based on the monitored motion at the bearings. In some of the earlier cases of self excited compressor whirling, the bearing preload was increased to improve the bearing stiffness to raise the critical speed. This bearing retrofit would result in lower whirl motion observed at the bearings but catastrophic shaft failure on startup.

A number of attempts were made to improve compressor stability by increasing the amount of bearing asymmetry. Although bearing asymmetry does improve rotor stability both in the cases of internal shaft friction and aerodynamic cross coupling, the vertical bearing stiffness can not exceed values in excess of the shaft modal stiffness. The design of multistage compressors in excess of 10 stages leads to shaft stiffness values of the order of 250,000 Lb/in.

With most 5 pad bearings with L/D ratios of 0.5, we obtain vertical bearing  $K_{yy}$  values well in excess of the ideal values. Under these conditions, bearing asymmetry is of no value in improving rotor stability. This has required a number of compressors to have squeeze film dampers installed. The squeeze film damper provides a soft support and an optimized damping value which may be considerably below the values obtained from the tilting pad bearing.

The paradox of the 5 pad bearing design is that many units may operate with constrained whirl motion by the simple procedure of reducing the bearing preload. This leads to larger motion observed at the bearings ( and possibly exceeding API codes). Hence preloads are increased, reducing bearing motion but leading to shaft rubs and failures. The further paradox of design is that high stability may be achieved by the initial design of a wider 4 pad bearing with load between pads. This design “floats” the shaft with a lower bearing stiffness.

Bearing asymmetry is not required for stabilization. This initial design approach is often rejected by the end user because it appears that the compressor may be operating near a critical speed in violation of API. This is a non issue since these higher critical speeds are so well damped that they are not excited or detected during operation. Thus the use of the critical speed map alone can lead to dangerous designs in an attempt to remove all apparent critical speeds from being near the operating speed.

## References

- Alford, J., 1965, “*Protecting Turbomachinery From Self-Excited Rotor Whirl*”, *Journal of Engineering For Power*, pp. 333-334
- Barrett, L. E., and Gunter, E. J. 1975, “*Steady State and Transient Analysis of a Squeeze film Damper*”, *NASA CR-2548*
- Chen, W. J., and Gunter, E. J. 2007, “*Introduction to Dynamics of Rotor-Bearing Systems*”, *Trafford Publishing*, ISBN: 978-1-4120-5190-3
- Gunter, E. J., 1966, “*Dynamic Stability of Rotor Bearing Systems*”, *NASA SP-113*
- Gunter, E. J. And Trumpler, P. R., 1969, “*The Influence of Internal Friction on the Stability of High Speed Rotors With Anisotropic Supports*”, *Journal of Engineering for Industry*, Nov., pp. 1105-1113
- Kimball, A. L. 1925, “*Internal Friction of Shaft Whirling*”, *General Electric Review*, Vol. 28 p. 554
- Kirk, R. G. And Donald, G. H., 1983, “*Design Criteria for Improved Stability of Centrifugal Compressors*”; *ASME Rotor Dynamical Instability*, AMD-Vol. 55
- Lund, J. W., 1964, “*Spring and Damping Coefficients for the Tilting Pad Journal Bearing*”, *ASLE Trans.*, Vol. 7, No. 4
- Lund, J. W., 1974, “*Stability and Damped Critical Speeds of a Flexible Rotor in Fluid Film Bearings*”, *ASME Journal of Engineering for Industry*
- Newkirk, B. L. 1924, “*Shaft Whipping*”, *General Electric Review*, Vol. 27, p. 169
- Nicholas, J. C., Gunter, E. J., Barrett, L. E., 1978, “*The Influence of Tilting Pad Bearing Characteristics on the Stability of High Speed Rotor Bearing Systems*”, *ASME Topics in Fluid Film Bearings and Rotor Bearing System Design and Optimization*, pp. 55-78
- Nicholas, J. C., Gunter, E. J., Allaire, P. A. 1979, “*Stiffness and Damping Coefficients for the Five-Pad Tilting-Pad Bearing*”, *ASLE Trans.*, Vol.22, No. 2
- Smith, K. J. 1975, “*An Operational History of Fractional Frequency Whirl*”, *Proceedings of The Fourth Annual Turbomachinery Symposium*, Texas A&M Univ. , pp. 115-125